



SCUOLA INTERNAZIONALE SUPERIORE DI STUDI AVANZATI

SISSA Digital Library

Entanglement entropy of two disjoint intervals in conformal field theory

Original

Entanglement entropy of two disjoint intervals in conformal field theory / Calabrese, Pasquale; Cardy, J; Tonni, Erik. - In: JOURNAL OF STATISTICAL MECHANICS: THEORY AND EXPERIMENT. - ISSN 1742-5468. - 2009:11(2009), pp. 1-37. [10.1088/1742-5468/2009/11/P11001]

Availability:

This version is available at: 20.500.11767/16552 since:

Publisher:

Published

DOI:10.1088/1742-5468/2009/11/P11001

Terms of use:

Testo definito dall'ateneo relativo alle clausole di concessione d'uso

Publisher copyright

IOP- Institute of Physics

This version is available for education and non-commercial purposes.

note finali coverpage

(Article begins on next page)

Entanglement entropy of two disjoint intervals in conformal field theory

Pasquale Calabrese¹, John Cardy², and Erik Tonni¹

¹Dipartimento di Fisica dell'Università di Pisa and INFN, Pisa, Italy.

²Oxford University, Rudolf Peierls Centre for Theoretical Physics, 1 Keble Road, Oxford, OX1 3NP, United Kingdom and All Souls College, Oxford.

Abstract.

We study the entanglement of two disjoint intervals in the conformal field theory of the Luttinger liquid (free compactified boson). $\text{Tr}\rho_A^n$ for any integer n is calculated as the four-point function of a particular type of twist fields and the final result is expressed in a compact form in terms of the Riemann-Siegel theta functions. In the decompactification limit we provide the analytic continuation valid for all model parameters and from this we extract the entanglement entropy. These predictions are checked against existing numerical data.

1. Introduction

The interest in quantifying the entanglement in extended quantum systems has been growing in recent times at an impressive rate, mainly because of its ability in detecting the scaling behaviour in proximity of quantum critical points (see e.g. Refs. [1, 2, 3, 4] as reviews). A particularly useful measure of entanglement in the ground-state of an extended quantum system is the entanglement entropy S_A . It is defined as follows. Let ρ be the density matrix of a system, which we take to be in the pure quantum state $|\Psi\rangle$, $\rho = |\Psi\rangle\langle\Psi|$. Let the Hilbert space be written as a direct product $\mathcal{H} = \mathcal{H}_A \otimes \mathcal{H}_B$. A 's reduced density matrix is $\rho_A = \text{Tr}_B \rho$. The entanglement entropy is the corresponding Von Neumann entropy

$$S_A = -\text{Tr} \rho_A \log \rho_A, \quad (1)$$

and analogously for S_B . When ρ corresponds to a pure quantum state $S_A = S_B$.

The entanglement entropy revealed to be an optimal indicator of the critical properties of an extended quantum system when A and B correspond to a spatial bipartition of the systems. Well-known and fundamental examples are critical one-dimensional systems in the case when A is an interval of length ℓ in an infinite line. In this case, the entanglement entropy follows the scaling [5, 6, 7]

$$S_A = \frac{c}{3} \log \frac{\ell}{a} + c'_1, \quad (2)$$

where c is the central charge of the associated conformal field theory (CFT) and c'_1 a non-universal constant. Away from the critical point, S_A saturates to a constant value [6] proportional to the logarithm of the correlation length [7]. This scaling allows to locate the position (where S_A diverges by increasing ℓ) and a main feature (by the value of the central charge c) of quantum critical points displaying conformal invariance.

The central charge is an ubiquitous and fundamental characteristic of the CFT, but it does not always identify unequivocally the universality class of the transition. A relevant class of relativistic quantum field theories are the so-called Luttinger liquids, which describe an enormous number of physical systems of experimental and theoretical interest. Just to quote a few, the one-dimensional Bose gases with repulsive interaction, the (anisotropic) Heisenberg spin chains, carbon nanotubes are all described by Luttinger liquid theory in their gapless phases. Via bosonization, all these models can be written as free bosonic field theories with $c = 1$. The different universality classes are distinguished by the compactification radius R of the bosonic field, that corresponds to experimentally measurable critical exponents.

The entanglement entropy of a single block of length ℓ , according to Eq. (2) is transparent to the value of the compactification radius, because it depends only on c . In Ref. [9] it has been shown that instead the entanglement entropy of disjoint intervals depends explicitly on R , and so it encodes universal properties of the CFT that are hidden in the entanglement of a single block. (Oppositely in 2D systems with conformal invariant wave-function, the entanglement entropy of a single region depends on R [10].) Eq. (2) in a CFT is calculated by a modification of the replica trick of disordered systems [5, 7]. In fact, one first calculates $\text{Tr} \rho_A^n$ for integral n , that results to be

$$\text{Tr} \rho_A^n = c_n \left(\frac{\ell}{a} \right)^{-\frac{c}{6}(n-1/n)}, \quad (3)$$

that is easily analytically continued to any complex value of n , and then $S_A = -\lim_{n \rightarrow 1} \partial_n \text{Tr} \rho_A^n$ gives Eq. (2). The reason of this way of proceeding is that for integral n , $\text{Tr} \rho_A^n$ is the partition function on an n -sheeted Riemann surface obtained by joining consecutively the n sheets along region A (see next section for details). We will refer to this surface as $\mathcal{R}_{n,N}$, where N is the number of disjoint intervals composing A . ($\mathcal{R}_{n,N}$ are fully defined by the $2N$ branch points u_j and v_j). In the case of a single interval, $\mathcal{R}_{n,1}$ is easily uniformised to the complex plane by a simple conformal mapping. Then the powerful tools of CFT give Eq. (3).

However, when the subsystem A consists of several disjoint intervals, the analysis becomes more complicated. In Ref. [7] (and also in [8]), based on a uniformising transformation mapping $\mathcal{R}_{n,N}$ into the complex plane, a general result for $\text{Tr} \rho_A^n$ has been given. However, this result is in general incorrect. In fact, the surface $\mathcal{R}_{n,N}$ has genus $(n-1)(N-1)$ and so for $N \neq 1$ cannot be uniformised to the complex plane (at the level of the transformation itself, this has been discussed in some details [11]). The case $n = N = 2$ has the topology of a torus, whose partition function depends on the whole operator content of the theory and not only on the central charge (see e.g. [12]). Consequently the simple formulas of Ref. [7] cannot be generally correct. The partition functions on Riemann surfaces with higher genus are even more complicated.

We consider here the case of two disjoint intervals $A = A_1 \cup A_2 = [u_1, v_1] \cup [u_2, v_2]$ defining the surface $\mathcal{R}_{n,2}$. By global conformal invariance $\text{Tr} \rho_A^n$ can be written as

$$\text{Tr} \rho_A^n \equiv Z_{\mathcal{R}_{n,2}} = c_n^2 \left(\frac{|u_1 - u_2| |v_1 - v_2|}{|u_1 - v_1| |u_2 - v_2| |u_1 - v_2| |u_2 - v_1|} \right)^{\frac{2}{3}(n-1/n)} \mathcal{F}_n(x), \quad (4)$$

where x is the four-point ratio (for real u_j and v_j , x is real)

$$x = \frac{(u_1 - v_1)(u_2 - v_2)}{(u_1 - u_2)(v_1 - v_2)}. \quad (5)$$

This can be written as

$$Z_{\mathcal{R}_{n,2}} = Z_{\mathcal{R}_{n,2}}^W \mathcal{F}_n(x), \quad (6)$$

where $Z_{\mathcal{R}_{n,2}}^W$ is the incorrect result in Ref. [7]. We normalised such that $\mathcal{F}_n(0) = 1$. The function $\mathcal{F}_n(x)$ depends explicitly on the full operator content of the theory and must be calculated case by case.

In Ref. [9], using old results of CFT on orbifolded space [13, 14], $\mathcal{F}_2(x)$ has been calculated for a free boson compactified on a circle of radius R

$$\mathcal{F}_2(x) = \frac{\theta_3(\eta\tau)\theta_3(\tau/\eta)}{[\theta_3(\tau)]^2}, \quad (7)$$

where τ is pure-imaginary, and is related to x via $x = [\theta_2(\tau)/\theta_3(\tau)]^4$. θ_ν are Jacobi theta functions. η is a universal critical exponent proportional to the square of the compactification radius R (in Luttinger liquid literature $\eta = 1/(2K)$).

The main result of this paper is $\mathcal{F}_n(x)$ for generic integral $n \geq 1$:

$$\mathcal{F}_n(x) = \frac{\Theta(0|\eta\Gamma)\Theta(0|\Gamma/\eta)}{[\Theta(0|\Gamma)]^2}, \quad (8)$$

where Γ is an $(n-1) \times (n-1)$ matrix with elements

$$\Gamma_{rs} = \frac{2i}{n} \sum_{k=1}^{n-1} \sin\left(\pi \frac{k}{n}\right) \beta_{k/n} \cos\left[2\pi \frac{k}{n}(r-s)\right], \quad (9)$$

and

$$\beta_y = \frac{F_y(1-x)}{F_y(x)}, \quad F_y(x) \equiv {}_2F_1(y, 1-y; 1; x). \quad (10)$$

η is exactly the same as above, while Θ is the Riemann-Siegel theta function

$$\Theta(z|\Gamma) \equiv \sum_{m \in \mathbf{Z}^{n-1}} \exp [i\pi m^t \cdot \Gamma \cdot m + 2\pi i m^t \cdot z], \quad (11)$$

with z a generic complex vector with $n-1$ components. $\Theta(0|\Gamma)$ for $n-1=1$ reduces to the Jacobi $\theta_3(\tau = i\beta_{1/2})$, and so Eq. (8) reproduces Eq. (7). In the above, and hereafter, the dot (\cdot) denotes the matrix product and the superscript t (t) the transposition. Eq. (8) is manifestly invariant under $\eta \rightarrow 1/\eta$, as numerically observed [9]. It is also invariant under $x \rightarrow 1-x$ (even if not manifest in this form). For $\eta = 1$ we have $\mathcal{F}_n(x) = 1$ and the result $Z_{\mathcal{R}_{2,N}}^W$ in [7] is then correct. This equality carries over to the analytic continuation and then to the entanglement entropy, confirming what observed numerically [9].

Unfortunately we have been not yet able to analytically continue this result to real n for general values of η and x , and so to obtain the entanglement entropy. However we managed to give asymptotic expressions for small and large η that compare well with numerics.

It is worth to recall that in the case of two intervals, the entanglement entropy measures only the entanglement of the two intervals with the rest of the system. It is *not* a measure of the entanglement of one interval with respect to the other, that instead requires the introduction of more complicated quantities because $A_1 \cup A_2$ is in a mixed state (see e.g. Refs. [15, 16] for a discussion of this and examples).

The paper is organized as follows. In Sec. 2 we recall how to obtain the entanglement entropy within CFT on Riemann surfaces and the usefulness of twist fields. In Sec. 3 we introduce the free compactified boson and fix all our notation. The following section 4 is the core of paper where Eq. (4) is derived. This section requires a good knowledge of CFT on orbifolds (to make the paper self-contained we also have a long Appendix A on this, where the results of Ref. [13] that we used are explained). The reader uninterested in the derivation can skip this section, to read directly Sec. 5 where a partial analytic continuation of Eq. (4) is performed and the consequences are discussed with particular attention to the comparison with the numerical results in Ref. [9]. Several appendices contain most of the technical parts of the paper.

2. Entanglement entropy and Riemann surfaces

Given a quantum field theory whose dynamics is described by the Hamiltonian H , the density matrix ρ in a thermal state at inverse temperature β may be written as a path integral in the imaginary time interval $(0, \beta)$

$$\rho(\{\phi_x\}|\{\phi'_{x'}\}) = Z^{-1} \int [d\phi(y, \tau)] \prod_x \delta(\phi(y, 0) - \phi'_{x'}) \prod_x \delta(\phi(y, \beta) - \phi_x) e^{-S_E}, \quad (12)$$

where $Z(\beta) = \text{Tr} e^{-\beta H}$ is the partition function, the euclidean action is $S_E = \int_0^\beta L d\tau$, with L the euclidean lagrangian. Here the rows and columns of the density matrix are labelled by the values of the fields at $\tau = 0, \beta$.

The normalisation factor of the partition function ensures that $\text{Tr} \rho = 1$, and is found by setting $\{\phi_x\} = \{\phi'_{x'}\}$ and integrating over these variables. In the path

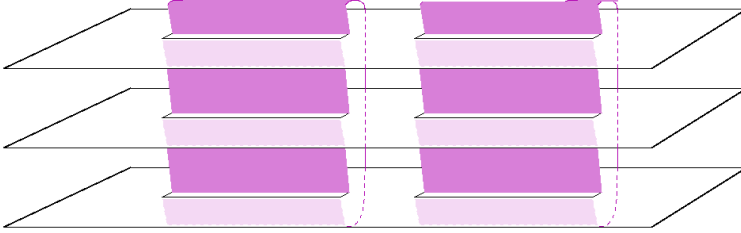


Figure 1. A representation of the Riemann surface $\mathcal{R}_{3,2}$.

integral, this has the effect of sewing together the edges along $\tau = 0$ and $\tau = \beta$ to form a cylinder of circumference β . Now let A be a subsystem consisting of the points x in the disjoint intervals $(u_1, v_1), \dots, (u_N, v_N)$. An expression for the reduced density matrix ρ_A is obtained from (12) by sewing together only those points x which are not in A . This has the effect of leaving open cuts, one for each interval (u_j, v_j) , along the line $\tau = 0$.

We may then compute $\text{Tr} \rho_A^n$, for any positive integer n , by making n copies of the above, labelled by an integer j with $1 \leq j \leq n$, and sewing them together cyclically along the the cuts so that $\phi_j(x, \tau = \beta^-) = \phi_{j+1}(x, \tau = 0^+)$ and $\phi_n(x, \tau = \beta^-) = \phi_1(x, \tau = 0^+)$ for all $x \in A$. This defines an n -sheeted Riemann surface depicted for $n = 3$ and in the case when A is formed by two disjoint intervals in Fig. 1. The partition function on this surface will be denoted by $Z_n(A)$ and so

$$\text{Tr} \rho_A^n = \frac{Z_n(A)}{Z^n}. \quad (13)$$

When the right hand side of the above equation has a unique analytic continuation to $\text{Re} n > 1$, its first derivative at $n = 1$ gives the required entropy

$$S_A = - \lim_{n \rightarrow 1} \frac{\partial}{\partial n} \text{Tr} \rho_A^n = - \lim_{n \rightarrow 1} \frac{\partial}{\partial n} \frac{Z_n(A)}{Z^n}. \quad (14)$$

Notice that even before taking the replica limit, these partition functions give the Rényi entropies

$$S_A^{(n)} = \frac{1}{1-n} \log \text{Tr} \rho_A^n. \quad (15)$$

Since the lagrangian density does not depend explicitly on the Riemann surface $\mathcal{R}_{n,N}$ as a consequence of its locality, it is expected that the partition function can be expressed as an object calculated from a model on the complex plane \mathbf{C} , where the structure of the Riemann surface is implemented through appropriate boundary conditions around the points with non-zero curvature. Consider for instance the simple Riemann surface $\mathcal{R}_{n,1}$ needed for the calculation of the entanglement entropy of a single interval $[u_1, v_1]$, made of n sheets sequentially joined to each other on the segment $x \in [u_1, v_1]$, $\tau = 0$. We expect that the associated partition function in a theory defined on the complex plane $z = x + i\tau$ can be written in terms of certain “fields” at $z = v_1$ and $z = u_1$.

The partition function (here $\mathcal{L}[\varphi](z, \bar{z})$ is the local lagrangian density)

$$Z_{\mathcal{R}_{n,N}} = \int [d\varphi]_{\mathcal{R}_{n,N}} \exp \left[- \int_{\mathcal{R}_{n,N}} dz d\bar{z} \mathcal{L}[\varphi](z, \bar{z}) \right], \quad (16)$$

essentially defines these fields (i.e. it gives their correlation functions, up to a normalisation independent of their positions). In order to work with local fields (see for an extensive discussion [17]), it is useful to move the intricate topology of the world-sheet (i.e. the space where the coordinates x, τ lie) $\mathcal{R}_{n,N}$ to the target space (i.e. the space where the fields lie). Let us consider a model formed by n independent copies of the original model. The partition function (16) can be re-written as the path integral on the complex plane

$$Z_{\mathcal{R}_{n,N}} = \int_{\mathcal{C}_{u_j, v_j}} [d\varphi_1 \cdots d\varphi_n]_{\mathbf{C}} \exp \left[- \int_{\mathbf{C}} dz d\bar{z} (\mathcal{L}[\varphi_1](z, \bar{z}) + \dots + \mathcal{L}[\varphi_n](z, \bar{z})) \right], \quad (17)$$

where with $\int_{\mathcal{C}_{u_j, v_j}}$ we indicated the *restricted* the path integral with conditions

$$\mathcal{C}_{u_j, v_j} : \quad \varphi_i(x, 0^+) = \varphi_{i+1}(x, 0^-), \quad x \in \bigcup_{j=1}^N [u_j, v_j], \quad i = 1, \dots, n, \quad (18)$$

where we identify $n + i \equiv i$. The lagrangian density of the multi-copy model is

$$\mathcal{L}^{(n)}[\varphi_1, \dots, \varphi_n](x, \tau) = \mathcal{L}[\varphi_1](x, \tau) + \dots + \mathcal{L}[\varphi_n](x, \tau),$$

so that the energy density is the sum of the energy densities of the n individual copies. Hence the expression (17) does indeed define local fields at $(u_1, 0)$ and $(v_1, 0)$ in the multi-copy model [17].

The local fields defined in (17) are examples of “twist fields”. Twist fields exist in a QFT model whenever there is a global internal symmetry σ (a symmetry that acts the same way everywhere in space, and that does not change the positions of fields): $\int dx d\tau \mathcal{L}[\sigma\varphi](x, \tau) = \int dx d\tau \mathcal{L}[\varphi](x, \tau)$. In the model with lagrangian $\mathcal{L}^{(n)}$, there is a symmetry under exchange of the copies. The twist fields defined by (17), which have been called *branch-point twist fields* [17], are twist fields associated to the two opposite cyclic permutation symmetries $i \mapsto i + 1$ and $i + 1 \mapsto i$ ($i = 1, \dots, n$, $n + 1 \equiv 1$). We can denote them simply by \mathcal{T}_n and $\tilde{\mathcal{T}}_n$, respectively

$$\mathcal{T}_n \equiv \mathcal{T}_\sigma, \quad \sigma : i \mapsto i + 1 \bmod n, \quad (19)$$

$$\tilde{\mathcal{T}}_n \equiv \mathcal{T}_{\sigma^{-1}}, \quad \sigma^{-1} : i + 1 \mapsto i \bmod n. \quad (20)$$

Notice that $\tilde{\mathcal{T}}_n$ can be identified with \mathcal{T}_{-n} . Thus for the n -sheeted Riemann surface along the set A made of N disjoint intervals $[u_j, v_j]$ we have

$$Z_{\mathcal{R}_{n,N}} \propto \langle \mathcal{T}_n(u_1, 0) \tilde{\mathcal{T}}_n(v_1, 0) \cdots \mathcal{T}_n(u_N, 0) \tilde{\mathcal{T}}_n(v_N, 0) \rangle_{\mathcal{L}^{(n)}, \mathbf{C}}. \quad (21)$$

This can be seen by observing that for $x \in [u_j, v_j]$, consecutive copies are connected through $\tau = 0$ due to the presence of $\mathcal{T}_n(v_j, 0)$, whereas for x in B , copies are connected to themselves through $\tau = 0$ because the conditions arising from the definition of $\mathcal{T}_n(u_j, 0)$ and $\tilde{\mathcal{T}}_n(v_j, 0)$ cancel each other. More generally, the identification holds for correlation functions in the model \mathcal{L} on \mathcal{R}

$$\langle \mathcal{O}(x, \tau; \text{sheet } i) \rangle_{\mathcal{L}, \mathcal{R}_{n,N}} = \frac{\langle \mathcal{T}_n(u_1, 0) \tilde{\mathcal{T}}_n(v_1, 0) \cdots \mathcal{T}_n(u_N, 0) \tilde{\mathcal{T}}_n(v_N, 0) \mathcal{O}_i(x, \tau) \rangle_{\mathcal{L}^{(n)}, \mathbf{C}}}{\langle \mathcal{T}_n(u_1, 0) \tilde{\mathcal{T}}_n(v_1, 0) \cdots \mathcal{T}_n(u_N, 0) \tilde{\mathcal{T}}_n(v_N, 0) \rangle_{\mathcal{L}^{(n)}, \mathbf{C}}}, \quad (22)$$

where \mathcal{O}_i is the field in the model $\mathcal{L}^{(n)}$ coming from the i^{th} copy of \mathcal{L} , and the ratio properly takes into account all the proportionality constants.

It is often useful to introduce the linear combinations of the basic fields

$$\tilde{\varphi}_k \equiv \sum_{j=1}^n e^{2\pi i \frac{k}{n} j} \varphi_j, \quad k = 0, 1, \dots, n-1, \quad (23)$$

that get multiplied by $e^{2\pi ik/n}$ on going around the twist operator, i.e. they diagonalize the twist

$$\mathcal{T}_n \tilde{\varphi}_k = e^{2\pi ik/n} \tilde{\varphi}_k, \quad \tilde{\mathcal{T}}_n \tilde{\varphi}_k = e^{-2\pi ik/n} \tilde{\varphi}_k. \quad (24)$$

Notice that when the basic fields φ_j are real then $\tilde{\varphi}_k^* = \tilde{\varphi}_{n-k}$. When the different values of k decouple, the total partition function is a product of the partition functions for each k . Thus also the twist fields can be written as products of fields acting only on $\tilde{\varphi}_k$

$$\mathcal{T}_n = \prod_{k=0}^{n-1} \mathcal{T}_{n,k}, \quad \tilde{\mathcal{T}}_n = \prod_{k=0}^{n-1} \tilde{\mathcal{T}}_{n,k}, \quad (25)$$

with $\mathcal{T}_{k,n} \tilde{\varphi}_{k'} = \tilde{\varphi}_{k'}$ if $k \neq k'$ and $\mathcal{T}_{k,n} \tilde{\varphi}_k = e^{2\pi ik/n} \tilde{\varphi}_k$. In terms of these fields, the partition function on the initial n -sheeted surface is

$$Z_{\mathcal{R}_{n,N}} = \prod_{k=0}^{n-1} \langle \mathcal{T}_{k,n}(u_1, 0) \tilde{\mathcal{T}}_{k,n}(v_1, 0) \dots \mathcal{T}_{k,n}(u_N, 0) \tilde{\mathcal{T}}_{k,n}(v_N, 0) \rangle_{\mathcal{L}^{(n)}, \mathbf{C}}. \quad (26)$$

This way of proceeding is very useful for free theories when the various k -modes decouple leading to Eq. (26). However, as we shall see soon, this is not straightforward for the problems we are considering here, because the compactification condition introduces a non trivial coupling between the k -modes.

3. Compactified boson on a Riemann surface

We consider a *complex* bosonic free field with Euclidean Lagrangian density

$$\mathcal{L} = \frac{g}{4\pi} |\nabla \varphi|^2. \quad (27)$$

The replicated theory is then ($\varphi_j = \varphi_{j,1} + i\varphi_{j,2}$)

$$\mathcal{L}^{(n)} = \frac{g}{4\pi} \sum_{j=1}^n (\partial_\mu \varphi_{j,1} \partial^\mu \varphi_{j,1} + \partial_\mu \varphi_{j,2} \partial^\mu \varphi_{j,2}) = \frac{g}{2\pi n} \sum_{k=0}^{n-1} (\partial_z \tilde{\varphi}_k \partial_{\bar{z}} \tilde{\varphi}_k^* + \partial_z \tilde{\varphi}_k^* \partial_{\bar{z}} \tilde{\varphi}_k),$$

with partition function

$$\begin{aligned} Z_{\mathcal{R}_{n,N}} &= \int_{\mathcal{C}} \left(\prod_{j=0}^{n-1} [d\varphi_j] \right) \exp \left\{ -\frac{g}{4\pi} \sum_{j=0}^{n-1} \int (\partial_\mu \varphi_{j,1} \partial^\mu \varphi_{j,1} + \partial_\mu \varphi_{j,2} \partial^\mu \varphi_{j,2}) d^2 z \right\} \\ &= \prod_{k=0}^{n-1} \int_{\mathcal{C}_k} [d\tilde{\varphi}_k] [d\tilde{\varphi}_k^*] \exp \left\{ -\frac{g}{2\pi n} \int (\partial_z \tilde{\varphi}_k \partial_{\bar{z}} \tilde{\varphi}_k^* + \partial_z \tilde{\varphi}_k^* \partial_{\bar{z}} \tilde{\varphi}_k) d^2 z \right\}, \end{aligned} \quad (28)$$

where \mathcal{C} stands for the restriction conditions in (18) and \mathcal{C}_k are the corresponding conditions on the fields $\tilde{\varphi}_k$.

The fields φ_j are free, but with each component compactified on a circle. Since the field is complex, the target space of \mathcal{L} is a torus with radii R_1 and R_2 . Encircling the branch points can lead to a non-trivial winding that can be written as (in the case of a branch point at the origin)

$$\varphi_j(e^{2\pi i} z, e^{-2\pi i} \bar{z}) = \varphi_{j-1}(z, \bar{z}) + R_1 m_{j,1} + i R_2 m_{j,2}, \quad m_{j,1}, m_{j,2} \in \mathbf{Z}, \quad (29)$$

where \mathbf{Z} is the set of integer numbers. In the following we will only consider equal compactification radii $R \equiv R_1 = R_2$. For the fields $\tilde{\varphi}_k$ these conditions read

$$\tilde{\varphi}_k(e^{2\pi i} z, e^{-2\pi i} \bar{z}) = e^{2\pi i \frac{k}{n}} \tilde{\varphi}_k(z, \bar{z}) + R \sum_{j=1}^n e^{2\pi i \frac{k}{n} j} m_j = \theta_k \tilde{\varphi}_k(z, \bar{z}) + R \sum_{j=1}^n \theta_k^j m_j, \quad (30)$$

where $m_j \in \mathbf{Z} + i\mathbf{Z}$ and we introduced $\theta_k \equiv e^{2\pi i \frac{k}{n}}$. Consequently, for a given $k \neq 0$, the target space for the fields $\tilde{\varphi}_k$ is compactified on a complicated ‘‘lattice’’ $R\Lambda_{k/n}$, where $\Lambda_{k/n}$ is the two dimensional set of vectors given by the generic combination through integer coefficients of the vectors $\{\theta_k, \theta_k^2, \dots, \theta_k^n\}$ (we recall that $\theta_k^n = 1$), i.e.

$$\Lambda_{\frac{k}{n}} = \left\{ q = \sum_{j=0}^{n-1} \theta_k^j m_j ; m_j \in \mathbf{Z} + i\mathbf{Z} \right\}. \quad (31)$$

This complicated structure of $\Lambda_{k/n}$ defining the space where the fields $\tilde{\varphi}_k$ are compactified is the precise reason why the approach based on Eq. (26) becomes difficult for the calculation of $Z_{\mathcal{R}_{n,2}}$. Few simple remarks on the structure of $\Lambda_{k/n}$ are in order. For fixed n , $\Lambda_{k/n} = \Lambda_{1-k/n}$. The vectors θ_k^j are not independent (e.g. $\sum_{j=0}^{n-1} \theta_k^j = 0$). In the following we will mainly use the results by Dixon et al. [13], but we have to stress here that there are a series of papers from late eighties about conformal field theories on orbifold (e.g. [14, 18, 19, 20]) that are very useful for the problem at hands and even for more complicated cases. The strategy of Ref. [13] to calculate these partition functions consists in splitting the field $\tilde{\varphi}_k$ in a classical and a quantum part $\tilde{\varphi}_k = \tilde{\varphi}_k^{\text{cl}} + \tilde{\varphi}_k^{\text{qu}}$. The evaluation of the Gaussian functional integral naturally divides into a sum over all classical solutions, times exponential of the quantum effective action. The classical solution takes into account the non-trivial topology of the target space as

$$\tilde{\varphi}_k^{\text{cl}}(e^{2\pi i} z, e^{-2\pi i} \bar{z}) = \theta_k^j \tilde{\varphi}_k^{\text{cl}}(z, \bar{z}) + v, \quad (32)$$

where $v \in R\Lambda_{k/n}$, while the quantum fluctuations are transparent to it

$$\tilde{\varphi}_k^{\text{qu}}(e^{2\pi i} z, e^{-2\pi i} \bar{z}) = \theta_k^j \tilde{\varphi}_k^{\text{qu}}(z, \bar{z}). \quad (33)$$

3.1. The two-point function and entanglement of a single interval

The two-point function of the twist fields for a complex field φ is [13] (see also Appendix A)

$$\langle \mathcal{T}_{k,n}(u) \tilde{\mathcal{T}}_{k,n}(v) \rangle \propto \frac{1}{|u-v|^{4\Delta_{k/n}}}, \quad (34)$$

where the dimensions of the twist fields read

$$\Delta_{\frac{k}{n}} = \bar{\Delta}_{\frac{k}{n}} = \frac{1}{2} \frac{k}{n} \left(1 - \frac{k}{n} \right). \quad (35)$$

Using Eq. (26), the partition function on $\mathcal{R}_{n,1}$ is

$$Z_{\mathcal{R}_{n,1}} = \prod_{k=0}^{n-1} Z_{k,n} = \prod_{k=0}^{n-1} \langle \mathcal{T}_{k,n}(u) \tilde{\mathcal{T}}_{k,n}(v) \rangle = \frac{c_n}{|u-v|^{4x_n}}, \quad (36)$$

with

$$x_n = \sum_{k=0}^{n-1} \Delta_{\frac{k}{n}} = \frac{1}{12} \left(n - \frac{1}{n} \right), \quad (37)$$

and we defined the normalisation constant c_n according to [7]. This is in agreement with the direct calculation [7] for central charge $c = 2$ because we are dealing with a complex field. For a *real field* the correlation function is the square root of the previous result, leading to an exponent x_n that is the half of above, in agreement with a $c = 1$ theory.

In the case of the two-point function it is then very easy to use Eq. (26) to obtain $Z_{\mathcal{R}_{n,1}}$. This is not the same for $Z_{\mathcal{R}_{n,2}}$ and we will adopt a slightly different strategy.

4. The four-point function of twist fields

Using Eq. (26) one is tempted to write the partition function on $\mathcal{R}_{n,2}$ as

$$Z_{\mathcal{R}_{n,2}} = \prod_{k=0}^{n-1} Z_{k,n} = \prod_{k=0}^{n-1} \langle \mathcal{T}_{k,n}(u_1, 0) \tilde{\mathcal{T}}_{k,n}(v_1, 0) \mathcal{T}_{k,n}(u_2, 0) \tilde{\mathcal{T}}_{k,n}(v_2, 0) \rangle. \quad (38)$$

This choice is consistent with the requirement that there should be no monodromy on going around both u_1 and v_1 or both u_2 and v_2 .

Using global conformal invariance the four-point function of twist fields can be generally written as

$$Z_{k,n}(u_1, v_1, u_2, v_2) \propto \left(\frac{|u_1 - u_2||v_1 - v_2|}{|u_1 - v_1||u_2 - v_2||u_1 - v_2||u_2 - v_1|} \right)^{4\Delta_{k/n}} \mathcal{G}_{k,n}(x), \quad (39)$$

where x is the four-point ratio given in Eq. (5). In the case of interest here x is real, but in the most general case can take any complex value (see also [11]). From Eq. (39) $Z_{\mathcal{R}_{n,2}}$ reduces to Eq. (4), after we normalise such that $\mathcal{F}_n(0) = 1$ (for $x \rightarrow 0$ $Z_{\mathcal{R}_{n,2}}$ is the product of two two-point functions previously calculated and normalised with c_n).

However, because of the compactification conditions of the field $\tilde{\varphi}_k$ Eq. (30), it is not easy to write the classical contributions to $Z_{k,n}$ and to avoid multiple-counting of the various classical solutions when summing over them. For this reason, we will adopt a mixed strategy. We will use Eq. (38) for the quantum part of $Z_{\mathcal{R}_{n,2}}$ that is transparent to the compactification conditions. This will allow to re-use the results of Ref. [13] without modification. For the classical contribution instead, we will sum over all the possible configurations of the fields φ_j that have easier compactification condition than $\tilde{\varphi}_k$.

4.1. The quantum part

The quantum part of the four point correlation (39) is independent from the compactification of the target space and it is responsible for the full scaling factor. It has been calculated in Ref. [13] and we report its derivation in the Appendix A. The final result is Eq. (A.30) that for real x becomes

$$Z_{k,n}^{\text{qu}} = \text{const} \left(\frac{|u_1 - u_2||v_1 - v_2|}{|u_1 - v_1||u_2 - v_2||u_1 - v_2||u_2 - v_1|} \right)^{4\Delta_{k/n}} \frac{1}{I_{k/n}(x)}, \quad (40)$$

where

$$I_{k/n}(x) \equiv 2F_{k/n}(x)F_{k/n}(1-x) = 2\beta_{k/n}[F_{k/n}(x)]^2, \quad (41)$$

where $F_y(x)$ and $\beta_{k/n}(x)$ are given in Eq. (10). Compared to Ref. [13] and to the appendix we have been stressing all the dependence on k/n of the various functions. Note that Eq. (41) is manifestly invariant for $x \rightarrow 1-x$. From this expression, the contribution of the quantum fluctuations to $Z_{\mathcal{R}_{n,2}}$ is readily obtained from Eq. (38).

4.2. The classical part

The value of the action on the classical solution of the equation of motion contributing to Z_k^{cl} has been derived in Ref. [13] for a general orbifolded theory. This derivation is reported in full details in the Appendix A. Here, for simplicity in the calculation and for physical reasons, we specialize to the case of x real. The action for a given classical configuration can be read from Eq. (A.39) in the appendix (fixing $\alpha_{k/n} = 0$ and using our normalisation for the action):

$$S_{\text{cl}} = \frac{2g\pi \sin(\pi k/n)}{n\beta_{k/n}} [|\xi_2|^2 + \beta_{k/n}^2 |\xi_1|^2], \quad (42)$$

where $\xi_1, \xi_2 \in R\Lambda_{k/n}$ are generic vectors of the target space lattice $R\Lambda_{k/n}$. At this point we could calculate $Z_{k,n}$ by summing over the vectors in the target space $R\Lambda_{k/n}$ given by Eq. (31). This computation would be very difficult. But not only, if in fact we would have been able to make this sum, the total partition function $Z_{\mathcal{R}_{n,2}}$ would not be given by Eq. (38) because some classical solutions would be counted more than once.

For all these reasons, we prefer to calculate the total partition function $Z_{\mathcal{R}_{n,2}}$ as the sum over all the classical configurations independently from the value of k . Thus, for a complex field compactified in both directions with the same radius, we have

$$Z_{\mathcal{R}_{n,2}} = \sum_{m \in \mathbf{Z}^{2n}} \prod_{k=0}^{n-1} Z_{k,n}^{\text{qu}} Z_{k,n}^{\text{cl}}, \quad (43)$$

and so in the total $\mathcal{F}_n(x)$ the scaling factor simplifies to give

$$\mathcal{F}_n(x) = \sum_{m \in \mathbf{Z}^{2n}} \prod_{k=0}^{n-1} \frac{\text{const}}{\beta_{k/n} [F_{k/n}(x)]^2} \exp \left\{ -\frac{2g\pi \sin(\pi \frac{k}{n})}{n} \left[|\xi_1|^2 \beta_{k/n} + \frac{|\xi_2|^2}{\beta_{k/n}} \right] \right\}. \quad (44)$$

Notice that we keep \sum_m out of \prod_k because, for each k , all the components of the vector $m \in \mathbf{Z}^{2n}$ (we are dealing with the complex φ_j 's; for real φ_j 's $m \in \mathbf{Z}^n$) are involved in the condition (30). The quantum part does not depend on m , and so we can factor it out as anticipated above:

$$\mathcal{F}_n(x) = \left[\prod_{k=0}^{n-1} \frac{\text{const}}{\beta_{\frac{k}{n}} [F_{\frac{k}{n}}(x)]^2} \right] \sum_{m \in \mathbf{Z}^{2n}} \prod_{k=0}^{n-1} \exp \left\{ \frac{-2g\pi \sin(\pi \frac{k}{n})}{n} \left[|\xi_1|^2 \beta_{\frac{k}{n}} + \frac{|\xi_2|^2}{\beta_{\frac{k}{n}}} \right] \right\}. \quad (45)$$

Given

$$\xi_p = R \sum_{l=0}^{n-1} \theta_k^l (m_{l,1}^{(p)} + i m_{l,2}^{(p)}), \quad p = 1, 2, \quad (46)$$

we have

$$\begin{aligned} |\xi_p|^2 &= R^2 \sum_{r,s=0}^{n-1} \left[\sum_{q=1,2} m_{r,q}^{(p)} \cos \left[2\pi \frac{k}{n} (r-s) \right] m_{s,q}^{(p)} \right. \\ &\quad \left. + (m_{r,1}^{(p)} m_{s,2}^{(p)} - m_{s,1}^{(p)} m_{r,2}^{(p)}) \sin \left[2\pi \frac{k}{n} (r-s) \right] \right] \\ &\equiv R^2 \left[\sum_{q=1,2} [m_q^{(p)}]^\dagger \cdot C_{\frac{k}{n}} \cdot m_q^{(p)} + \sum_{r,s=0}^{n-1} (m_{r,1}^{(p)} m_{s,2}^{(p)} - m_{s,1}^{(p)} m_{r,2}^{(p)}) (S_{\frac{k}{n}})_{rs} \right], \quad (47) \end{aligned}$$

where $m_q^{(p)} \in \mathbf{Z}^n$ and

$$\left(C_{\frac{k}{n}}\right)_{rs} \equiv \cos \left[2\pi \frac{k}{n}(r-s)\right], \quad \left(S_{\frac{k}{n}}\right)_{rs} \equiv \sin \left[2\pi \frac{k}{n}(r-s)\right]. \quad (48)$$

Notice that $C_{\frac{k}{n}}$ is invariant for $k \leftrightarrow n-k$, while $S_{\frac{k}{n}}$ changes sign. For this reason, when summing over k in the total partition function at fixed r, s , the two terms with $S_{\frac{k}{n}}$ and $S_{\frac{n-k}{n}}$ cancel out. This fundamental simplification does not happen if we consider only the partition sum at fixed k . The remaining two sums over $m_q^{(p)} \in \mathbf{Z}^n$ factorize and we have

$$\begin{aligned} Z_{\text{cl}} &= \left[\sum_{m \in \mathbf{Z}^n} \prod_{k=0}^{n-1} \exp \left\{ -\frac{2\pi g}{n} R^2 \sin \left(\pi \frac{k}{n} \right) \left[\beta_{k/n} m^t \cdot C_{\frac{k}{n}} \cdot m + \frac{m^t \cdot C_{\frac{k}{n}} \cdot m}{\beta_{k/n}} \right] \right\} \right]^2 \\ &= \left[\sum_{m \in \mathbf{Z}^n} \exp \left\{ i\pi \left[m^t \cdot \Omega \cdot m + m^t \cdot \tilde{\Omega} \cdot m \right] \right\} \right]^2, \end{aligned} \quad (49)$$

where the matrices Ω and $\tilde{\Omega}$ are

$$\Omega_{rs} \equiv 2gR^2 \frac{i}{n} \sum_{k=0}^{n-1} \sin \left(\pi \frac{k}{n} \right) \beta_{\frac{k}{n}} \cos \left[2\pi \frac{k}{n}(r-s) \right], \quad (50)$$

$$\tilde{\Omega}_{rs} \equiv 2gR^2 \frac{i}{n} \sum_{k=0}^{n-1} \sin \left(\pi \frac{k}{n} \right) \frac{1}{\beta_{\frac{k}{n}}} \cos \left[2\pi \frac{k}{n}(r-s) \right], \quad (51)$$

and the indices r and s run over $1, \dots, n$. We remark that the term corresponding to $k=0$ is zero, thus we can deal with $\sum_{k=1}^{n-1}$ in these definitions. All elements of these matrices have vanishing real part.

Given a $G \times G$ symmetric complex matrix Γ with positive imaginary part, the Riemann-Siegel theta function is defined as in Eq. (11). However, Ω and $\tilde{\Omega}$ have one common eigenvector with vanishing eigenvalue that is $(1, 1, \dots, 1)$. The sum in Eq. (49) is then divergent and cannot be written as $\Theta(0|\Omega)\Theta(0|\tilde{\Omega})$. After diagonalizing these matrices, we will see that is easy to adsorb this divergence in the normalisation factor.

The eigenvalues of Ω and $\tilde{\Omega}$ are

$$\omega_q = 2gR^2 \sin \left(\pi \frac{q}{n} \right) i\beta_{q/n}, \quad \tilde{\omega}_q = 2gR^2 \sin \left(\pi \frac{q}{n} \right) \frac{i}{\beta_{q/n}}, \quad q = 1, \dots, n, \quad (52)$$

For $q=n$ (or equivalently $q=0$) the eigenvalue is vanishing, and then the imaginary parts of Ω and $\tilde{\Omega}$ are not positive definite. Notice also that $\omega_q = \omega_{n-q}$ and $\tilde{\omega}_q = \tilde{\omega}_{n-q}$.

The matrices Ω and $\tilde{\Omega}$ have a common eigenbasis whose normalised eigenvectors can be written as

$$(y_q)_r \equiv \frac{e^{2\pi i \frac{q}{n} r}}{\sqrt{n}}, \quad q, r = 1, \dots, n. \quad (53)$$

Thus, the $n \times n$ complex matrix U whose elements are $U_{rs} \equiv (y_r)_s$ is unitary and it simultaneously diagonalizes Ω and $\tilde{\Omega}$, i.e.

$$U\Omega U^\dagger = \left(\begin{array}{ccc|c} \omega_1 & & & 0 \\ & \ddots & & \vdots \\ & & \omega_{n-1} & 0 \\ \hline 0 & & 0 & 0 \end{array} \right) \equiv \Omega_{\text{d}}, \quad U\tilde{\Omega}U^\dagger = \left(\begin{array}{ccc|c} \tilde{\omega}_1 & & & 0 \\ & \ddots & & \vdots \\ & & \tilde{\omega}_{n-1} & 0 \\ \hline 0 & & 0 & 0 \end{array} \right) \equiv \tilde{\Omega}_{\text{d}}.$$

In order to extract the divergence from (49), we introduce a regulator by setting $i\epsilon$ ($0 < \epsilon \ll 1$) instead of 0 for the last eigenvalue i.e.

$$\Omega_{d,\epsilon} \equiv \left(\begin{array}{ccc|c} \omega_1 & & & 0 \\ & \ddots & & \vdots \\ & & \omega_{n-1} & 0 \\ \hline 0 & & 0 & i\epsilon \end{array} \right), \quad \tilde{\Omega}_{d,\epsilon} \equiv \left(\begin{array}{ccc|c} \tilde{\omega}_1 & & & 0 \\ & \ddots & & \vdots \\ & & \tilde{\omega}_{n-1} & 0 \\ \hline 0 & & 0 & i\epsilon \end{array} \right). \quad (54)$$

We introduce \hat{U} as the restriction of U to the first $n-1$ eigenvectors (i.e. we have dropped the eigenvector generating the kernel) $\hat{U}_{qr} \equiv U_{qr}$ for $q, r = 1, \dots, n-1$. We remark that \hat{U} is not unitary. We write the vector of integer numbers m as $m = M + \hat{m}$, with M belonging to the kernel (i.e. proportional to $(1, \dots, 1)$) and \hat{m} to the space orthogonal to it. Using the orthogonality of M and \hat{m} , we have

$$m^\dagger \cdot \Omega \cdot m = (\bar{U}m)^\dagger \cdot \Omega_d \cdot (Um) = \left[\lim_{\epsilon \rightarrow 0} (\bar{U}M)^\dagger \cdot \Omega_{d,\epsilon} \cdot (UM) \right] + (\bar{U}\hat{m})^\dagger \cdot \Omega_d \cdot (U\hat{m})$$

where we explicitly used that in the space orthogonal to the kernel the product gives a finite result (and then the sum will be finite). We have the same relation for $\tilde{\Omega}$. We can re-organize the sum in Eq. (49), summing before on the numbers spanned by \hat{m} (that give a finite Θ function in an $n-1$ dimensional space) and after the diverging sum over the kernel. We finally find

$$Z_{cl} = \left[\left(\lim_{\epsilon \rightarrow 0} \frac{1}{n\epsilon} \right) \Theta(0|\eta\Gamma) \Theta(0|\eta\tilde{\Gamma}) \right]^2, \quad (55)$$

where we defined

$$\eta\Gamma \equiv \hat{U}^\dagger \left(\begin{array}{ccc} \omega_1 & & \\ & \ddots & \\ & & \omega_{n-1} \end{array} \right) \hat{U}, \quad \eta\tilde{\Gamma} \equiv \hat{U}^\dagger \left(\begin{array}{ccc} \tilde{\omega}_1 & & \\ & \ddots & \\ & & \tilde{\omega}_{n-1} \end{array} \right) \hat{U}, \quad (56)$$

which are symmetric and have positive imaginary parts and therefore provide well defined Riemann-Siegel theta functions.

The matrices $\eta\Gamma$ and $\eta\tilde{\Gamma}$ are Ω and $\tilde{\Omega}$ respectively with the last line and row dropped, i.e.

$$\Gamma_{rs} = \frac{2i}{n} \sum_{k=1}^{n-1} \sin\left(\pi \frac{k}{n}\right) \beta_{k/n} \cos\left[2\pi \frac{k}{n}(r-s)\right] = \frac{2}{n} \sum_{k=1}^{n-1} \sin\left(\pi \frac{k}{n}\right) i\beta_{k/n} e^{2\pi i \frac{k}{n}(r-s)},$$

$$\tilde{\Gamma}_{rs} = \frac{2i}{n} \sum_{k=1}^{n-1} \sin\left(\pi \frac{k}{n}\right) \frac{1}{\beta_{k/n}} \cos\left[2\pi \frac{k}{n}(r-s)\right] = \frac{2}{n} \sum_{k=1}^{n-1} \sin\left(\pi \frac{k}{n}\right) \frac{i}{\beta_{k/n}} e^{2\pi i \frac{k}{n}(r-s)},$$

where $r, s = 1, \dots, n-1$. We introduced the matrices Γ and $\tilde{\Gamma}$, in such a way that they do not depend on R and we defined

$$\eta = gR^2, \quad (57)$$

that is exactly the same as in Ref. [9], while the normalisation of R is different.

Thus, taking (45) and (55), adsorbing the divergence for $\epsilon \rightarrow 0$ into the constant, we have

$$\mathcal{F}_n(x) = \text{const} \frac{[\Theta(0|\eta\Gamma) \Theta(0|\eta\tilde{\Gamma})]^2}{\prod_{k=1}^{n-1} \beta_{k/n} [F_{k/n}(x)]^2} = \text{const} \frac{[\Theta(0|\eta\Gamma) \Theta(0|\eta\tilde{\Gamma})]^2}{\prod_{k=1}^{n-1} F_{k/n}(x) F_{k/n}(1-x)}. \quad (58)$$

This expression is manifestly invariant for $x \rightarrow 1-x$ because under this transformation $\beta_{k/n} \leftrightarrow 1/\beta_{k/n}$ and so $\Gamma \leftrightarrow \tilde{\Gamma}$.

In order to fix properly the normalisation constant (given by $\mathcal{F}_n(0) = 1$) and to show explicitly the invariance under $\eta \rightarrow 1/\eta$, it is worth to manipulate this expression. Using Poisson resummation formula, in Appendix B we show the following identity

$$\Theta(0|\eta\tilde{\Gamma}) = \eta^{-\frac{n-1}{2}} \left(\prod_{k=0}^{n-1} \beta_{k/n} \right)^{\frac{1}{2}} \Theta(0|\Gamma/\eta). \quad (59)$$

We finally have

$$\mathcal{F}_n(x) = \text{const} \frac{[\Theta(0|\eta\Gamma) \Theta(0|\eta\tilde{\Gamma})]^2}{\prod_{k=1}^{n-1} \beta_{k/n} [F_{k/n}(x)]^2} = \left[\frac{\Theta(0|\eta\Gamma) \Theta(0|\Gamma/\eta)}{\prod_{k=1}^{n-1} F_{k/n}(x)} \right]^2 \quad (60)$$

where we fixed the constant by requiring that for $\mathcal{F}_n(0) = 1$ (we used that for $x \rightarrow 0$, $F_{k/n}(0) = 1$, and $\beta_{k/n} \rightarrow +\infty$; furthermore $\Theta(0|\Gamma)$ goes to 1 for $\beta_{k/n} \rightarrow \infty$). We have thus written \mathcal{F}_n in a way that is manifestly symmetric for the exchange $\eta \leftrightarrow 1/\eta$.

A last manipulation can be done by using

$$[\Theta(0|\Gamma)]^2 = \prod_{k=1}^{n-1} F_{k/n}(x), \quad (61)$$

proved in Appendix C. This finally leads to the square of Eq. (8), in fact this equation is valid for a complex field compactified in both directions with the same radius. The real field corresponds to the square root of the previous result. This final manipulation allows to manifestly show that $\mathcal{F}_n(x)|_{\eta=1} = 1$ identically.

It is also worth to mention that we wrote the partition function over a n -sheeted Riemann surface in terms of a Riemann-Siegel theta function defined with a matrix of dimension $n-1$ that is exactly the genus of the covering surface.

4.3. Special cases

4.3.1. $n = 2$. In this case the matrix Γ is just 1 by 1, and so $\Theta(0|\Gamma)$ is a standard Jacobi θ_3 function. Thus Eq. (60) ($\tau_{1/2} = i\beta_{1/2}$)

$$\mathcal{F}_2(x) = \left[\frac{\theta_3(\tau_{1/2}\eta)\theta_3(\tau_{1/2}/\eta)}{\theta_3^2(\tau_{1/2})} \right]^2, \quad (62)$$

where we used that $F_{1/2}(x) = \theta_3^2(\tau_{1/2})$. This is exactly the square of the result in Ref. [9] as it must be.

4.3.2. $n = 3$. First we observe that there is only one τ because $\tau_{1/3} = \tau_{2/3}$. We have

$$\Gamma = \frac{\tau_{1/3}}{\sqrt{3}} \begin{pmatrix} 2 & -1 \\ -1 & 2 \end{pmatrix} = \frac{1}{\sqrt{2}} \begin{pmatrix} 1 & -1 \\ 1 & 1 \end{pmatrix} \begin{pmatrix} \gamma/3 & 0 \\ 0 & \gamma \end{pmatrix} \frac{1}{\sqrt{2}} \begin{pmatrix} 1 & -1 \\ 1 & 1 \end{pmatrix}^t, \quad (63)$$

where $\gamma = \sqrt{3}\tau_{1/3}$. Since these matrices are written in terms of integers only, this allows to write $\Theta(0|\eta\Gamma)$ as a sum of θ_3 and θ_2 and finally using the duplication formulas to prove the following identity

$$[\Theta(0|\eta\Gamma)]^2 = \frac{1}{2} \left[\theta_2(\eta\gamma)^2 \theta_2\left(\frac{\eta\gamma}{3}\right)^2 + \theta_3(\eta\gamma)^2 \theta_3\left(\frac{\eta\gamma}{3}\right)^2 + \theta_4(\eta\gamma)^2 \theta_4\left(\frac{\eta\gamma}{3}\right)^2 \right]. \quad (64)$$

The same is clearly true for $\Theta(0|\Gamma/\eta)$, obtaining

$$\mathcal{F}_3(x) = \frac{1}{4[F_{1/3}(x)]^4} \left[\theta_2(\eta\gamma)^2 \theta_2\left(\frac{\eta\gamma}{3}\right)^2 + \theta_3(\eta\gamma)^2 \theta_3\left(\frac{\eta\gamma}{3}\right)^2 + \theta_4(\eta\gamma)^2 \theta_4\left(\frac{\eta\gamma}{3}\right)^2 \right] \\ \times \left[\theta_2\left(\frac{\gamma}{\eta}\right)^2 \theta_2\left(\frac{\gamma}{3\eta}\right)^2 + \theta_3\left(\frac{\gamma}{\eta}\right)^2 \theta_3\left(\frac{\gamma}{3\eta}\right)^2 + \theta_4\left(\frac{\gamma}{\eta}\right)^2 \theta_4\left(\frac{\gamma}{3\eta}\right)^2 \right].$$

4.3.3. $n = 4$. Using tricks similar to the case $n = 3$, it is possible to write $\Theta(0|\Gamma)^2$ for $n = 4$ as a sum of 6 terms that are products of three θ_i (with different τ 's now, because in general $\tau_{2/4} \neq \tau_{1/4} = \tau_{3/4}$). This expression is however very long and not illuminating.

4.4. Decompactification regime

For fixed x , in the limit of large η we have $\Theta(0|\eta\Gamma) = 1 + \dots$ and

$$\Theta(0|\Gamma/\eta) = \frac{1}{\sqrt{\det(-i\Gamma/\eta)}} (1 + \dots) = \frac{\eta^{(n-1)/2}}{\sqrt{\det(-i\Gamma)}} (1 + \dots), \quad (65)$$

where \dots denotes vanishing terms as $\eta \rightarrow \infty$. Thus

$$\mathcal{F}_n(x) = \frac{\eta^{n-1}}{\prod_{k=1}^{n-1} F_{k/n}(x) F_{k/n}(1-x)}, \quad (66)$$

recovering the correct quantum result Eq. (A.30) with the proper η dependent normalisation (we used $\det(-i\Gamma) = \prod_{k=1}^{n-1} \beta_{k/n}$ and $\beta_{k/n} = F_{k/n}(1-x)/F_{k/n}(x)$).

Note that, using the symmetry $\eta \leftrightarrow 1/\eta$, the same formula gives also the answer for $\eta \rightarrow 0$.

4.5. Small x regime

Another case when the final result can be written in terms of simple functions is the expansion for small x , corresponding to two far distant intervals (and by symmetry $x \rightarrow 1-x$ also for x close to 1, corresponding to close intervals).

For $x \rightarrow 0$ the expansion of $\beta_{k/n}$ is

$$\beta_{\frac{k}{n}} = -\frac{\sin\left(\frac{\pi k}{n}\right)}{\pi} \left(\log x + f_{\frac{k}{n}} + \sum_{l=1}^{\infty} p_l \left(\frac{k}{n}\right) x^l \right), \quad f_{\frac{k}{n}} \equiv 2\gamma_E + \psi\left(\frac{k}{n}\right) + \psi\left(1 - \frac{k}{n}\right),$$

where γ_E is the Euler gamma, $\psi(z) \equiv \Gamma'(z)/\Gamma(z)$ is the Polygamma function (also know as digamma function) and $p_l(z)$ is a polynomial of degree $2l$, whose explicit expression is not needed. Plugging this expansion in the Riemann-Siegel theta function we obtain

$$\Theta(0|\eta\Gamma) = 1 + \sum_{m \in \mathbf{Z}^{n-1} \setminus \{\vec{0}\}} x^{\eta \frac{2}{n} \sum_{k=1}^{n-1} \sin\left(\frac{\pi k}{n}\right)^2 m^{\mathbf{t}} \cdot C_{k/n} \cdot m} e^{\eta \frac{2}{n} \sum_{k=1}^{n-1} \sin\left(\frac{\pi k}{n}\right)^2 f_{k/n} m^{\mathbf{t}} \cdot C_{k/n} \cdot m} (1 + O(x)), \quad (67)$$

where the matrix $C_{k/n}$ is defined in (48). In this expansion the leading term is provided by those vectors $m \in \mathbf{Z}^{n-1} \setminus \{\vec{0}\}$ which minimize the expression

$$\frac{2}{n} \sum_{k=1}^{n-1} \sin\left(\frac{\pi k}{n}\right)^2 m^{\mathbf{t}} \cdot C_{k/n} \cdot m = \sum_{j=1}^{n-1} m_j^2 - \sum_{j=1}^{n-2} m_j m_{j+1}. \quad (68)$$

This expression is obviously minimized by all vectors of the form $m_{l,\pm}^{\dagger} \equiv (0, \dots, 0, \pm 1, \dots, \pm 1, 0, \dots, 0)$, with l contiguous ± 1 's. At fixed $l = 1, \dots, n-1$, there are $2(n-l)$ of such vectors for which the expression (68) is 1. In order to evaluate the coefficient in front of the leading term, we observe that

$$m_{l,\pm}^{\dagger} \cdot C_{k/n} \cdot m_{l,\pm} = \sum_{r,s=1}^l \left(C_{\frac{k}{n}} \right)_{rs} = \left(\frac{\sin(\pi \frac{k}{n} l)}{\sin(\pi \frac{k}{n})} \right)^2. \quad (69)$$

Using the following integral representation for the digamma function

$$\psi(y) + \gamma_E = \int_0^{\infty} \frac{e^{-t} - e^{-yt}}{1 - e^{-t}} dt, \quad (70)$$

exchanging the order of sum and integral and then performing the latter, after simple algebra we find

$$\frac{2}{n} \sum_{k=1}^{n-1} \sin\left(\pi \frac{k}{n}\right)^2 f_{k/n} m_{l,\pm}^{\dagger} \cdot C_{k/n} \cdot m_{l,\pm} = -\log \left[2n \sin\left(\pi \frac{l}{n}\right) \right]^2. \quad (71)$$

Now, assuming $\eta \neq 1$, in the ratio of Riemann-Siegel theta functions occurring in $\mathcal{F}_n(x)$ the leading term is given by the minimum between η and $1/\eta$, that we indicate as $\alpha = \min(\eta, 1/\eta)$. Therefore we get the small x behavior of the scaling function

$$\mathcal{F}_n(x) = 1 + x^{\alpha} \sum_{l=1}^{n-1} \frac{2(n-l)}{[2n \sin(\pi \frac{l}{n})]^{2\alpha}} + \dots = 1 + 2 \left(\frac{x}{4n^2} \right)^{\alpha} \sum_{l=1}^{n-1} \frac{l}{[\sin(\pi \frac{l}{n})]^{2\alpha}} + \dots, \quad (72)$$

where the dots denote higher order terms in x . Note that for $n=2$ this results reduces to $\mathcal{F}_2(x) = 1 + 2(x/16)^{\min(\eta, 1/\eta)} + \dots$, as already found in [9]. We stress, once more, that this expansion is valid only for $\eta \neq 1$, in fact for $\eta = 1$ the denominator in $\mathcal{F}_n(x)$ (that is of order $O(x)$) cancels exactly the numerator.

4.6. Different compactification radii

In this manuscript we mainly consider the case of a complex boson compactified in both directions with the same radius, because it has more physical applications and also to lighten the notation. However it is straightforward to generalize to the case with different compactification radii (at least for real four-point ratio x). The only change is that the target space is given by the product of two circles with different radii $R_1 \neq R_2$. Eq. (46) now becomes

$$\xi_p = \sum_{l=0}^{n-1} \theta_k^l \left(R_1 m_{l,1}^{(p)} + i R_2 m_{l,2}^{(p)} \right). \quad (73)$$

The only (minimal) changes compared to the case of equal radii are in the computation in Eqs. (47). Repeating the straightforward algebra we have

$$\begin{aligned} |\xi_p|^2 &= \sum_{r,s=0}^{n-1} \theta_k^r \bar{\theta}_k^s \left(R_1 m_{r,1}^{(p)} + i R_2 m_{r,2}^{(p)} \right) \left(R_1 m_{s,1}^{(p)} - i R_2 m_{s,2}^{(p)} \right) \\ &= \sum_{r,s=0}^{n-1} \left[\left(C_{\frac{k}{n}} \right)_{rs} \left(R_1^2 m_{r,1}^{(p)} m_{s,1}^{(p)} + R_2^2 m_{r,2}^{(p)} m_{s,2}^{(p)} \right) - R_1 R_2 \left(S_{\frac{k}{n}} \right)_{rs} \left(m_{r,2}^{(p)} m_{s,1}^{(p)} - m_{r,1}^{(p)} m_{s,2}^{(p)} \right) \right] \\ &= \left[R_1^2 m_1^{(p)\dagger} \cdot C_{\frac{k}{n}} \cdot m_1^{(p)} + R_2^2 m_2^{(p)\dagger} \cdot C_{\frac{k}{n}} \cdot m_2^{(p)} + R_1 R_2 \text{tr} \left(A S_{\frac{k}{n}} \right) \right]. \end{aligned} \quad (74)$$

The important point is that the term in $R_1 R_2$ is still vanishing and so the classical part of the action corresponds to the one of two independent real bosons. Note that this property is not completely trivial because the compactification conditions are not on the fields $\tilde{\varphi}_k$. The divergences due to $k = 0$ are removed as before, arriving to the final expression

$$\mathcal{F}_n(x) = \left[\frac{\Theta(0|\eta_1\Gamma)\Theta(0|\Gamma/\eta_1)}{\Theta(0|\Gamma)^2} \right] \left[\frac{\Theta(0|\eta_2\Gamma)\Theta(0|\Gamma/\eta_2)}{\Theta(0|\Gamma)^2} \right], \quad (75)$$

where $\eta_j \equiv gR_j^2$, the matrix Γ is defined in Eq. (9) and the normalization has been chosen such that $\mathcal{F}_n(0) = 1$.

5. The analytic continuation and the entanglement entropy

In order to obtain the entanglement entropy we should be able to analytically continue Eq. (8) to general complex value of n and, only after, take the derivative for $n \rightarrow 1$. The definition of the Riemann-Siegel theta function makes this program hard, because it explicitly involves summations involving a matrix of dimensions $(n-1) \times (n-1)$ that are not obviously continued to real values of n . One should find a different representation of the same function which is manipulable and we have been unable to do it. However, it is possible to analytically continue the denominator of Eq. (8). This is not only a first step towards the full analytic continuation, but it provides all the answer in the decompactification regime (Eq. 66), allowing to give precise predictions for $\eta \ll 1$ and $\eta \gg 1$.

The logarithm of the denominator in Eq. (60) is a sum over $k = 1 \dots n-1$, which involves analytic functions of k . In this case it is possible to use the residue theorem to write the sum as an integral in the complex plane of $\log F_{k/n}(x)$ times a function that has poles only for integer values of k and over a contour that encircles all of them. A useful representation of this is

$$D_n(x) = \sum_{k=1}^{n-1} \log F_{k/n}(x) = \int_{\mathcal{C}} \frac{dz}{2\pi i} \pi \cot(\pi z) \log F_{z/n}(x), \quad (76)$$

where \mathcal{C} can be chosen as the rectangular contour $(n-iL, n+iL, iL, -iL)$ (because $\log F_0(x) = \log F_1(x) = 0$ and $\cot(z)$ has no poles for $\text{Im}z \neq 0$). We can now change variable $z/n \rightarrow z$ to obtain

$$D_n(x) = n \int_{\mathcal{C}'} \frac{dz}{2i} \cot(\pi z n) \log F_z(x), \quad (77)$$

and \mathcal{C}' is the re-scaled rectangle $(1-iL, 1+iL, iL, -iL)$. This simple formula provides the desired analytic continuation. Notice that all the poles of the integrand in the strip $0 \leq \text{Re}z \leq 1$ are on the real axis. Then, if the argument of the integral would decay quickly enough for $\text{Im}z \rightarrow \pm\infty$, we could send $L \rightarrow \infty$, ignoring the contribution of the horizontal pieces and remaining only with the vertical ones. This is unfortunately not the case, because the integrand is increasing when $L \rightarrow \infty$.

We can however take the derivative wrt n in the contour integral. This leads to

$$D'_1(x) \equiv - \left. \frac{\partial D_n(x)}{\partial n} \right|_{n=1} = \int_{\mathcal{C}'} \frac{dz}{2i} \frac{\pi z}{\sin^2 \pi z} \log F_z(x). \quad (78)$$

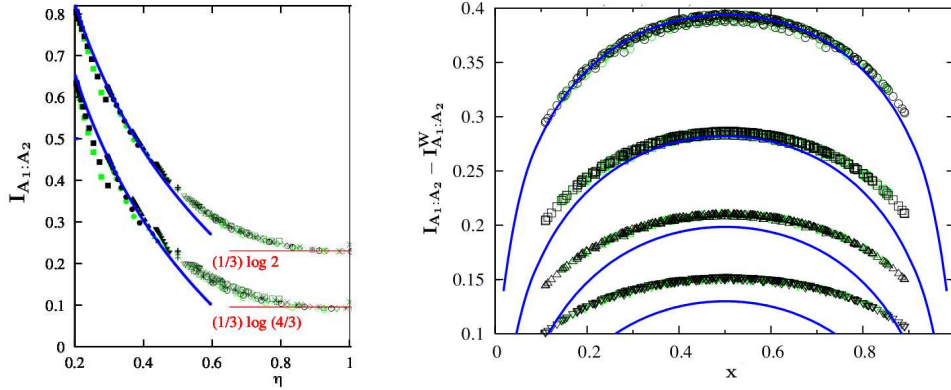


Figure 2. Mutual information $I_{A_1:A_2}^{(1)}$ for the XXZ model. All numerical data are extracted from Ref. [9]. Left: $I_{A_1:A_2}^{(1)}$ for $x = 1/2$ (top curve) and $x = 1/4$ (bottom curve) as function of η . The continuous curve is the decompactification result Eq. (82). Right: $I_{A_1:A_2}^{(1)}$ at fixed η as function of x . The top curve corresponds to $\eta = 0.295$ small enough to agree for all considered x with Eq. (82). The other curves correspond to higher values of η , when the small η approximation loses validity.

In this integral, the horizontal contribution is vanishing for $L \rightarrow \infty$ and so only the vertical ones are left. Because of the periodicity of the integrand these two contributions are equal and so

$$D'_1(x) = - \int_{-i\infty}^{i\infty} \frac{dz}{i} \frac{\pi z}{\sin^2 \pi z} \log F_z(x). \quad (79)$$

Such integral is easily evaluated numerically for any x . For $x = 1/2$ it is possible to get an analytic result with a different method (see Appendix D) that agrees with the value calculated numerically. To cross check our results in the appendix we also provide the analytic continuation as perturbation series in x . Despite the asymptotic character of the perturbative expansion, it provides a very good approximation for all $x \leq 1/2$.

5.1. The entanglement entropy in the decompactification regime

From Eq. (66) and using the result above for the analytic continuation, we have that the entanglement entropy for a *real* boson in the decompactification regime is

$$S_A(\eta \ll 1) - S_A^W \simeq \frac{1}{2} \ln \eta - \frac{D'_1(x) + D'_1(1-x)}{2}, \quad (80)$$

where S_A^W is the result in Ref. [7]. The same result obviously holds for $\eta \gg 1$ with the replacement $\eta \rightarrow \eta^{-1}$.

This should be compared with the numerical results for the XXZ model by Furukawa et al. [9], where the entanglement of the XXZ chain for generic values of the anisotropy Δ and magnetic field (always in the gapless phase) has been calculated by direct diagonalization for systems up to 30 spins. In the absence of the magnetic field, η is related to the anisotropy by $\eta = 1 - (\arccos \Delta)/\pi$, while for non-zero h_z a

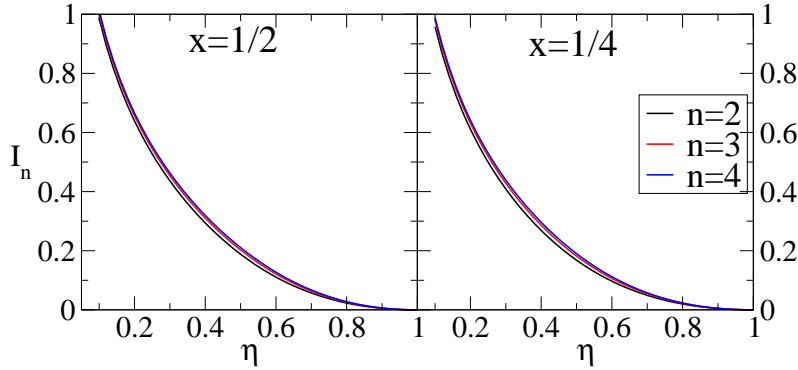


Figure 3. I_n in Eq. (85) as function of η for x constant $x = 1/2$ (left panel) and $x = 1/4$ (right panel). In each plot the three curves corresponds to different values of $n = 2, 3, 4$ (from bottom to top).

closed formula for η does not exist and must be calculated numerically as explained in [9]. The main results have been written in terms of the Rényi mutual informations

$$I_{A_1:A_2}^{(n)} = S_{A_1}^{(n)} + S_{A_2}^{(n)} - S_{A_1 \cup A_2}^{(n)} = -\frac{n+1}{6n} c \log(1-x) + \frac{1}{n-1} \log \mathcal{F}_n(x), \quad (81)$$

where A_1 and A_2 are the two intervals composing $A = A_1 \cup A_2$. For $n = 1$ the data (reported also in Fig. 2), when plotted in terms of x collapse on a single curve, confirming the validity of the scaling form. In Ref. [9], only $I_{A_1:A_2}^{(2)}$ has been compared with the available CFT prediction Eq. (7). However, for $n = 2$, the collapse of the data is worse than the one for $I_{A_1:A_2}^{(1)}$ because of the strong oscillating corrections to the scaling of the Rényi entropies (analogous to the ones observed for a single interval [23, 22]). However, the agreement was rather satisfactory, considering the small system sizes and the oscillations.

Here we are in position to offer a first prediction for the von-Neumann mutual information $I_{A_1:A_2}^{(1)}$. The numerical data from Ref. [9] are reported in Fig. 2. The prediction in the decompactification regime is

$$I_{A_1:A_2}^{(1)}(\eta \ll 1) - I_{A_1:A_2}^{(1),W} \simeq -\frac{1}{2} \ln \eta + \frac{D_1'(x) + D_1'(1-x)}{2}, \quad (82)$$

where again $I_{A_1:A_2}^{(1),W}$ is the result of Ref. [7]. This prediction, for various values of η and x are reported in Fig. 2. In the left panel it has been reported the mutual information as function of η at fixed $x = 1/2, 1/4$. On the scale of this plot, the decompactification prediction reproduces the numerical data up to $\eta \sim 0.4$ and for larger values clearly deviates. In the right panel of Fig. 2 it is reported the x dependence of the mutual information at fixed η . Again for the smallest value $\eta = 0.295$ the decompactification approximation is valid for all x . Increasing η this is no longer true, but it works better for $x \sim 1/2$, while it quickly deteriorates moving from the central point.

5.2. The entanglement entropy for small x

We can obtain the analytic continuation also in the small x regime starting from the results in Sec. 4.5. We need to analytically continue $\mathcal{F}_n(x)$ in Eq. (72) valid for $\eta \neq 1$.

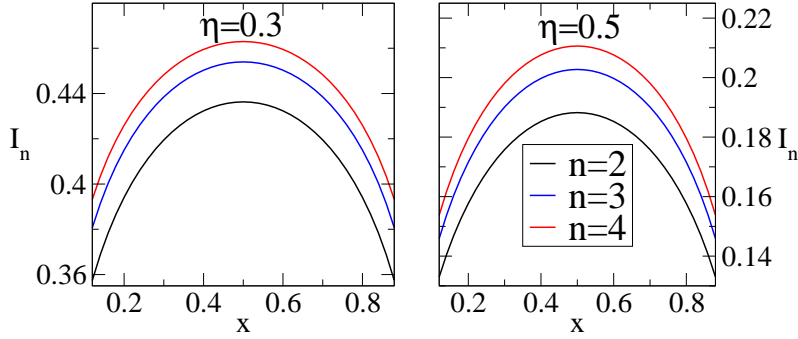


Figure 4. I_n in Eq. (85) as function of x at constant $\eta = 0.3$ (left panel) and $\eta = 0.5$ (right panel). In each plot the three curves correspond to different values of $n = 2, 3, 4$ (from bottom to top).

Calling $\alpha = \min(\eta, 1/\eta)$, we can write $\mathcal{F}_n(x)$ as

$$\mathcal{F}_n(x) = 1 + 2n \left(\frac{x}{4n^2} \right)^\alpha P_n + \dots \quad \text{with} \quad P_n = \sum_{l=1}^{n-1} \frac{l/n}{[\sin(\pi l/n)]^{2\alpha}}. \quad (83)$$

Within this definition we have that, after analytically continuing, the contribution to the entanglement entropy is (we recall that $P_1 = 0$)

$$S_A - S_A^W = -\mathcal{F}'_1(x) = 2^{1-2\alpha} x^\alpha P'_1 + \dots \quad (84)$$

The most important consequence is that for small x the entanglement entropy has a power law behavior in x with an exponent that is always α for any $\eta \neq 1$. The multiplicative coefficient of this power law is exactly calculated by analytically continuing P_n . This derivation is however rather cumbersome and it is reported in Appendix D.3. The dependence of P'_1 from η can be read in the plot in Fig. D1.

5.3. Results for integer n

In this section we report some explicit results for integer n . These are shown in Figs. 3, 4, and 5, where we always plot the quantity

$$I_n = \frac{1}{n-1} \log \mathcal{F}_n(x), \quad (85)$$

that contributes directly to the Rényi entropy and mutual information. After analytic continuation, this quantity has also a smooth limit to $n = 1$, and so it is ideal to show some general properties.

In Fig. 3, following Ref. [9] (also left panel in Fig. 2), we plotted I_n as function of η with x kept constant to $x = 1/2$ (left panel) and $x = 1/4$ (right panel). In each plot the three curves correspond to different values of $n = 2, 3, 4$. It is evident that on the scale of the plot, the differences between various n are tiny. This means (if nothing really strange happens in the analytical continuation) that also the equivalent plot for I_1 (contributing to the entanglement entropy) will be qualitatively and quantitatively similar. In particular, to appreciate the differences between various values of n on these kinds of plots, the numerical results must be extremely precise. In fact, the results in Ref. [9] (reported also in the left panel of Fig. 2) are practically indistinguishable from those in Fig. 3.

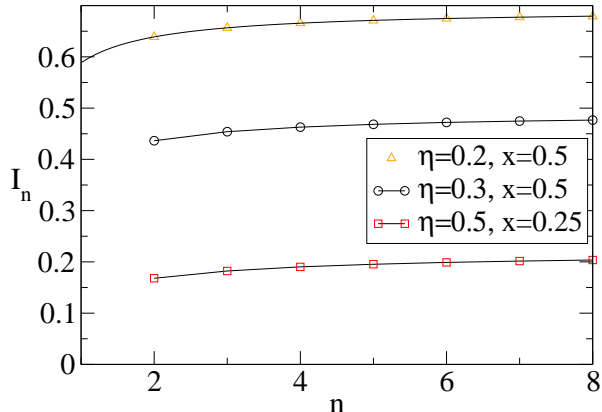


Figure 5. I_n in Eq. (85) as function of n at constant η and x . The points at n integer are real data, the lines are only guide for the eyes, except the top one that is the analytic continuation for small η .

A more effective way to show the differences between various n is to plot I_n as a function of x keeping η constant, as in Fig. 4. Because of the reduced scale of variation of I_n with x , the differences between the various n are evident and guessing quantitative features of the analogous plot for the analytic continuation at $n = 1$ is not recommended. When n increases the corresponding value of I_n increases, in qualitative agreement with the numerical results of Ref. [9] (see Fig. 3 there). As already stated, a direct comparison of the numerical and analytically results is quantitatively impossible because of the strong oscillating corrections to the scaling in the XXZ model.

Finally in Fig. 5 we keep constant both η and x and show the dependence of I_n on n . On the scale of the plot, the n -dependence is small. However, before making wrong considerations about a smooth behaviour in taking the limit for $n \rightarrow 1$ in the analytic continuation, it is worth to have a look at the exact results we have for small η . We then consider $\eta = 0.2$ and $x = 1/2$ (top curve in Fig. 5). The points are the exact results for n integer from Eq. (8), while the continuous line is the analytic continuation given by Eqs. (D.5) and (66). For such small value of η , the decompactification formula is indistinguishable from the exact data. The analytic continuation displays a pronounced binding of the curve for $1 < n < 2$, that makes difficult any naive extrapolation from the data with $n \geq 2$.

6. Conclusions

We considered the entanglement of two disjoint intervals $A = [u_1, v_1] \cup [u_2, v_2]$ in the ground-state of the CFT of the Luttinger liquid (free compactified boson). We presented a complete analysis for $\text{Tr} \rho_A^n$ for any integer n , leading to the result we anticipated in the introduction Eq. (4). We have not yet been able to analytically continue the numerator of this expression to obtain the entanglement entropy. However, in the decompactification regime when the exponent η is very small or very large, we calculated explicitly the entanglement entropy and the associated mutual information leading to Eq. (82). Our predictions agree well with the numerical computations of Furukawa et al. [9] for the XXZ model that is described by this CFT.

The error in Ref. [7] also carries over to the case of semi-infinite systems, where now half of the points are the images ones. Also in this case a still unknown function $\tilde{\mathcal{F}}_n(x)$ corrects the result. However, this error does not impact on the later application

by two of us of these methods to studying the time-dependence of the entanglement entropy following a quantum quench [32]. This is because in this case only the limiting behaviour, when the various cross-ratios are either small or large, is needed, and this is insensitive to the precise form of $\mathcal{F}_n(x)$. Likewise, as far as we are aware, all the other conclusions of Ref. [32] remain valid. Instead the function $\tilde{\mathcal{F}}_n(x)$ affects some results in Ref. [33] for local quantum quenches, that however are easily corrected using the formulas for general four-point correlation functions presented in the same paper. See for a more detailed discussion the review [3].

The analytic continuation of $\mathcal{F}_n(x)$ to general real n remains the most interesting open problem. However, there are several other issues that deserve to be discussed. Firstly it is difficult to check directly our predictions for $\text{Tr}\rho_A^n$ for integer n with the numerical data in Ref. [9]. This because, as observed already in [9] for $n = 2$, there are strong oscillating corrections to the scaling making the comparison hard, if not impossible, for the system sizes accessible by exact diagonalization. There are several possible way-outs to this problem. One could try to describe these corrections analytically, as done for the single interval [22] and adding them to the leading contribution, but this seems to be very difficult. Alternatively one could use different numerical methods to access largest system sizes. Density matrix renormalisation group (eventually in the recent version proposed in Ref. [15] to deal with a similar issue) could be effective. Furthermore, the Monte-Carlo based approach by Caraglio and Gliozzi [11] applies to the case of integer n . This could then be used to test our predictions for models showing smaller oscillations (even in the same universality class). One can also wonder whether Eq. (4) is enough to calculate analytically the full spectrum of eigenvalues of the reduced density matrix. In fact, in Ref. [34] it has been shown that this can be calculated by knowing $\text{Tr}\rho_A^n$ for integer n only.

A few comments are also in order. In Ref. [24, 25, 26, 27, 29], the entanglement entropy for two disjoint intervals has been calculated for free fermionic theories, that after bosonization always correspond to a compactified boson with $\eta = 1/2$ [12]. However, it has been found that the entanglement entropy is given by $Z_{\mathcal{R}_{n,2}}^W$, apparently in contrast with the numerical calculation in Ref. [9] and what found here. The details of this apparent disagreement are still not completely understood, but they should be traced back to the different boundary conditions that result from constructing the reduced density matrix for spin or fermion variables. For the Ising model numerical computations [28] also show a good agreement with $Z_{\mathcal{R}_{n,2}}^W$. Also in this case, it is likely that the deviations from $Z_{\mathcal{R}_{n,2}}^W$ should be attributed to the choice of the variables used in constructing the reduced density matrix. (In fact, the calculations in the spin variables [35] show numerically and analytically that $Z_{\mathcal{R}_{n,2}}^W$ is not correct.) Finally holographic calculations in AdS/CFT correspondence [30, 31] considering the classical limit in the gravity sector, also found $Z_{\mathcal{R}_{n,2}}^W$. It would be interesting to understand how the correct result might arise from taking into account the quantum effects on the gravity side.

We close this paper by discussing the case with $N > 2$ disjoint intervals. As far as we are aware there are no firm results in the literature. By global conformal invariance we have

$$\text{Tr}\rho_A^n = c_n^N \left(\frac{\prod_{j < k} (u_k - u_j)(v_k - v_j)}{\prod_{j,k} (v_k - u_j)} \right)^{(c/6)(n-1/n)} \mathcal{F}_{n,N}(\{x\}). \quad (86)$$

For $\mathcal{F}_{n,N}(\{x\}) = 1$ this is the incorrect result of Ref. [7] (note a typo in the

denominator). $\{x\}$ stands for the collection of $2N - 3$ independent ratios that can be built with $2N$ points. Some old results from CFT on orbifolds in Refs. [14, 19] could be useful to calculate $\mathcal{F}_{n,N}(\{x\})$ for a compactified boson.

Acknowledgments

We thank S. Furukawa, F. Gliozzi and V. Pasquier for useful discussions and correspondence. We thank all authors of Ref. [9] for allowing us to use their numerical results. JC thanks Benjamin Hsu for early discussions on this topic. ET is also grateful to Hong Liu, J. McGreevy, and A. Scardicchio. This work was supported in part by EPSRC grant EP/D050952/1. PC benefited of a travel grant from ESF (INSTANS activity).

Appendix A. Correlation functions of twist fields and \mathbf{Z}_n orbifolds

In a order to make this paper self-contained, in this appendix we review the results of Ref. [13] for CFT on orbifold spaces that we used. In particular we will show how to obtain Eqs. (40) and (42). As we have stressed in the main text twist fields exist in a QFT whenever there is a global internal symmetry. An orbifold is obtained by identifying points of the target space through a given equivalence relation, leading automatically to a global symmetry and so to the presence of twist fields (that is why Ref. [13] contains the main ingredients for our calculations). To be explicit a D dimensional orbifold \mathbf{R}^D/S is obtained by identifying points of the target space \mathbf{R}^D through an equivalence relation

$$X' \sim X, \quad \text{if} \quad X' = \theta X + v \equiv gX, \quad g = (\theta, v), \quad (\text{A.1})$$

where θ is a rotation and v is a vector of \mathbf{R}^D . The set of the pairs $S = \{(\theta, v)\}$ defining the orbifold is called *space group*, while the subgroup $\Lambda = \{g = (1, v)\} \subset S$, made by the translations only, is called *lattice* Λ of S . A simple example of orbifold is obtained by identifying points in the target space with opposite signs $X \sim -X$. This gives rise to so-called \mathbf{Z}_2 orbifolds. A \mathbf{Z}_n orbifold is generated by a rotation θ of order n (i.e. $\theta^n = 1$) and its space group S is given by the pairs (θ^j, v) with $j = 0, 1, 2, \dots, n-1$ and v runs over an even dimensional lattice Λ . Among the conjugacy classes making up the partition of S , we distinguish the ones of the form $\{(1, \theta^j v_0)\}$ (v_0 is a fixed vector of \mathbf{R}^D), which contain only the translation elements of S and therefore describe the winding sectors. Instead, elements like (θ^j, v) with $j = 1, 2, \dots, n-1$ and $v \in \Lambda$ belong to classes like

$$\{(\theta^j, \theta^r v_0 + (1 - \theta^j)u); r \in \mathbf{Z}, u \in \Lambda\}, \quad (\text{A.2})$$

which describe the twisted sectors. Notice that, for each $j = 1, 2, \dots, n-1$, there are many conjugacy classes of the form $\{(\theta^j, v)\}$ with v belonging to different subsets (cosets) of the lattice Λ . Thus, as for the twist fields associated to the \mathbf{Z}_n orbifold, each of them is characterized by two indices: the index $j = 1, 2, \dots, n-1$ of the twisted sector of the Hilbert space and another index ε labelling the conjugacy class within that sector. The twist-fields in our problems are exactly the same that appears in \mathbf{Z}_n orbifolds, but since we do not have identifications of points the index ε can be only zero and will be ignored in the following.

Let us go back to our main goal, that is the calculation of the four-point function of twist fields. Let us consider a complex field $X(z, \bar{z})$ defined on the worldsheet given

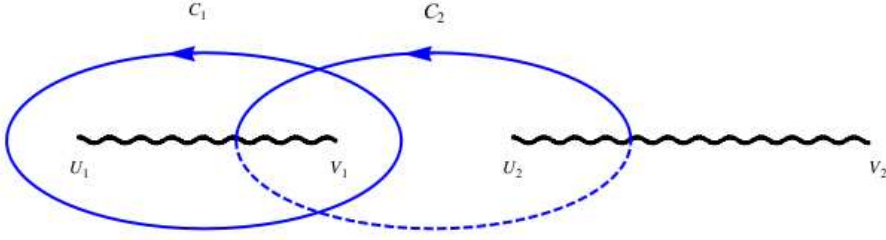


Figure A1. The two closed loops \mathcal{C}_1 and \mathcal{C}_2 we considered as basis. The different sheets are indicated as solid vs dashed lines.

by the Riemann sphere (this is one of the $\tilde{\varphi}_k$ in the main text). The occurrence of the twist field in the origin tells us how the field X is rotated and translated when it is carried around this point in the worldsheet, i.e.

$$X(e^{2\pi i}z, e^{-2\pi i}\bar{z}) = \theta^j X(z, \bar{z}) + v, \quad (\text{A.3})$$

where v is a vector of the coset. The phase rotation θ^j of X is the monodromy of the field. In order to make this definition meaningful, the field X must be complex.

When X is taken around a set of points where different twist-fields are placed, it is rotated and translated according to the product of the space group elements associated with the different twist fields. The relevant circuits to consider in order to completely fix the boundary conditions are the ones enclosing a collection of twist fields with *net twist zero*, namely the loops along which the field X acquires no phase. Such paths \mathcal{C} are called *closed loops*. Two example of closed loops that we will use in the following are reported in Fig. A1.

Splitting the field $X = X_{\text{cl}} + X_{\text{qu}}$ into its classical part X_{cl} and its quantum counterpart X_{qu} , we impose (A.3) by requiring that

$$X_{\text{cl}}(e^{2\pi i}z, e^{-2\pi i}\bar{z}) = \theta^j X_{\text{cl}}(z, \bar{z}) + v, \quad (\text{A.4})$$

and

$$X_{\text{qu}}(e^{2\pi i}z, e^{-2\pi i}\bar{z}) = \theta^j X_{\text{qu}}(z, \bar{z}), \quad (\text{A.5})$$

namely X_{qu} ignores the translations in the space group. Thus, for any closed loop \mathcal{C} , we have

$$\Delta_{\mathcal{C}} X_{\text{qu}} = \oint_{\mathcal{C}} dz \partial_z X_{\text{qu}} + \oint_{\mathcal{C}} d\bar{z} \partial_{\bar{z}} X_{\text{qu}} = 0, \quad (\text{A.6})$$

and

$$\Delta_{\mathcal{C}} X_{\text{cl}} = \oint_{\mathcal{C}} dz \partial_z X_{\text{cl}} + \oint_{\mathcal{C}} d\bar{z} \partial_{\bar{z}} X_{\text{cl}} = v, \quad (\text{A.7})$$

where now v is not the same of (A.4), but it is a vector of Λ depending on the twist fields enclosed by \mathcal{C} . For the twist field $\mathcal{T}_{k,n}$ we have

$$v \in (1 - \theta)\Lambda, \quad (\text{A.8})$$

where, compared to Ref. [13], we fixed $f_{\varepsilon_1} = f_{\varepsilon_2} = 0$, because we have only the trivial fixed point 0. The requirements (A.6) and (A.7) are the *global monodromy conditions*.

Let us take $\theta = e^{2\pi ik/n}$ (i.e. θ_k in the main text) to be the rotation by an angle $2\pi k/n$ for a fixed $k \in \{1, 2, \dots, n-1\}$. In all this appendix we will consider fixed values of k and n , and so there is no ambiguity in denoting with \mathcal{T} and $\tilde{\mathcal{T}}$ what in the text we called $\mathcal{T}_{k,n}$ and $\tilde{\mathcal{T}}_{k,n}$ (i.e. the twist field associated to θ and θ^{-1} respectively and that in [13] are called σ_+ and σ_-). We fix $j = 1$ in Eqs. (A.4) and (A.5). Also all other quantities will loose the subscripts k and n etc. We are interested to the following four point function

$$Z = \langle \mathcal{T}(z_1, \bar{z}_1) \tilde{\mathcal{T}}(z_2, \bar{z}_2) \mathcal{T}(z_3, \bar{z}_3) \tilde{\mathcal{T}}(z_4, \bar{z}_4) \rangle = \int [dX][d\bar{X}] e^{-S[X, \bar{X}]}, \quad (\text{A.9})$$

where the action for the complex field X reads

$$S[X, \bar{X}] = \frac{1}{4\pi} \int (\partial_z X \partial_{\bar{z}} \bar{X} + \partial_{\bar{z}} X \partial_z \bar{X}) d^2 z. \quad (\text{A.10})$$

Separating the classical contribution from the quantum part, we can write

$$Z = Z_{\text{qu}} \sum_{\langle X_{\text{cl}} \rangle} e^{-S_{\text{cl}}}, \quad (\text{A.11})$$

where $S_{\text{cl}} \equiv S[X_{\text{cl}}, \bar{X}_{\text{cl}}]$. The classical part in (A.11) is given by the sum over the possible configurations of the classical field, which are characterized by (A.7).

Following [13], let us start by considering the Green function in the presence of four twist-fields

$$g(z, w; z_i) = \frac{\langle -\frac{1}{2} \partial_z X \partial_w \bar{X} \mathcal{T}(z_1) \tilde{\mathcal{T}}(z_2) \mathcal{T}(z_3) \tilde{\mathcal{T}}(z_4) \rangle}{\langle \mathcal{T}(z_1) \tilde{\mathcal{T}}(z_2) \mathcal{T}(z_3) \tilde{\mathcal{T}}(z_4) \rangle}. \quad (\text{A.12})$$

Imposing that for $z \rightarrow w$ we have $g(z, w; z_j) \sim (z-w)^{-2}$ and that for $z \rightarrow z_j$ we have $g(z, w; z_j) \sim (z-z_j)^{-k/n}$ and $g(z, w; z_j) \sim (z-z_j)^{-(1-k/n)}$ for j odd and even respectively (and the opposite for $w \rightarrow z_j$), we can write $g(z, w; z_j)$ as

$$g(z, w; z_i) = \omega_k(z) \omega_{n-k}(w) \left[\frac{k}{n} \frac{(z-z_1)(z-z_3)(w-z_2)(w-z_4)}{(z-w)^2} + \left(1 - \frac{k}{n}\right) \frac{(z-z_2)(z-z_4)(w-z_1)(w-z_3)}{(z-w)^2} + A(z_j, \bar{z}_j) \right], \quad (\text{A.13})$$

where

$$\omega_k(z) = [(z-z_1)(z-z_3)]^{-k/n} [(z-z_2)(z-z_4)]^{-(1-k/n)}, \quad (\text{A.14})$$

and $A(z_j, \bar{z}_j)$ is a constant (in z and w) that contains the dependence of $g(z, w; z_i)$ on the antiholomorphic coordinates and must be determined by global monodromy conditions.

Let us now consider the limit $w \rightarrow z$

$$\lim_{w \rightarrow z} [g(z, w) - (z-w)^{-2}] = \frac{1}{2} \frac{k}{n} \left(1 - \frac{k}{n}\right) \left(\frac{1}{z-z_1} + \frac{1}{z-z_3} - \frac{1}{z-z_2} - \frac{1}{z-z_4} \right)^2 + \frac{A(z_j, \bar{z}_j)}{(z-z_1)(z-z_2)(z-z_3)(z-z_4)}. \quad (\text{A.15})$$

This is exactly the expectation value of the insertion of the stress energy tensor of the field X in the four-point correlation function. By taking the limit $z \rightarrow z_j$ for any j , one reads the dimensions of the twist fields \mathcal{T} and $\tilde{\mathcal{T}}$

$$\Delta_{\frac{k}{n}} = \bar{\Delta}_{\frac{k}{n}} = \frac{1}{2} \frac{k}{n} \left(1 - \frac{k}{n}\right), \quad (\text{A.16})$$

as anticipated in the main text. Let us also introduce the auxiliary correlation function

$$h(\bar{z}, w; z_j) = \frac{\langle -\frac{1}{2}\partial_{\bar{z}}X\partial_w\bar{X}\mathcal{T}(z_1)\tilde{\mathcal{T}}(z_2)\mathcal{T}(z_3)\tilde{\mathcal{T}}(z_4)\rangle}{\langle \mathcal{T}(z_1)\tilde{\mathcal{T}}(z_2)\mathcal{T}(z_3)\tilde{\mathcal{T}}(z_4)\rangle} = B(z_j, \bar{z}_j)\bar{\omega}_{n-k}(\bar{z})\omega_{n-k}(w),$$

where the rhs above comes from the same considerations as before, but the singular terms in $(z-w)$ do not occur because $h(\bar{z}, w; z_j)$ is regular in this variable.

In order to lighten the notation it is convenient hereafter to employ the following conformal map

$$z \rightarrow \frac{(z_1 - z)(z_3 - z_4)}{(z_1 - z_3)(z - z_4)} \quad (\text{A.17})$$

which sends z_1, z_2, z_3 and z_4 into 0, x , 1 and ∞ respectively, where x is the four-point ratio ($z_{ij} = z_i - z_j$)

$$x \equiv \frac{z_{12}z_{34}}{z_{13}z_{24}}, \quad x(1-x) = \frac{z_{21}z_{43}z_{41}z_{32}}{z_{31}^2z_{42}^2}. \quad (\text{A.18})$$

After this mapping the dependence on z_i in the various functions reduces to the dependence on the ratio x and its complex conjugate \bar{x} only.

Taking the limit $z \rightarrow x$ in Eq. (A.15), one finds the following differential equation for the quantum part of the correlation function

$$\partial_x \ln Z_{\text{qu}}(x, \bar{x}) = -2\Delta_{k/n} \left(\frac{1}{x} - \frac{1}{1-x} \right) - \frac{A(x, \bar{x})}{x(1-x)}, \quad (\text{A.19})$$

The global monodromy conditions allow to determine $A(x, \bar{x})$. In terms of the functions g and h they read

$$0 = \oint_{\mathcal{C}} dz g(z, w) + \oint_{\mathcal{C}} d\bar{z} h(\bar{z}, w). \quad (\text{A.20})$$

Dividing by $\omega_{n-k}(w)$ and letting $w \rightarrow \infty$ this gives

$$A(x, \bar{x}) \oint_{\mathcal{C}} dz \omega_k(z) + B(x, \bar{x}) \oint_{\mathcal{C}} d\bar{z} \bar{\omega}_k(\bar{z}) = - \left(1 - \frac{k}{n} \right) \oint_{\mathcal{C}} dz (z-x) \omega_k(z). \quad (\text{A.21})$$

These integrals are valid for all closed loops. We choose as a basis of these loops the two ones depicted in Fig. A1, that suffices to determine $A(x, \bar{x})$.

All these integrals are easily calculated giving [13]

$$\oint_{\mathcal{C}_1} dz \omega_k(z) = 2\pi i e^{-i\pi k/n} F(x), \quad \oint_{\mathcal{C}_2} dz \omega_k(z) = 2\pi i F(1-x), \quad (\text{A.22})$$

$$\oint_{\mathcal{C}_1} d\bar{z} \bar{\omega}_{n-k}(\bar{z}) = 2\pi i e^{-i\pi k/n} \bar{F}(\bar{x}), \quad \oint_{\mathcal{C}_2} d\bar{z} \bar{\omega}_{n-k}(\bar{z}) = -2\pi i \bar{F}(1-\bar{x}), \quad (\text{A.23})$$

$$- \left(1 - \frac{k}{n} \right) \oint_{\mathcal{C}_1} dz (z-x) \omega_k(z) = 2\pi i e^{-i\pi k/n} x(1-x) \frac{dF(x)}{dx}, \quad (\text{A.24})$$

$$- \left(1 - \frac{k}{n} \right) \oint_{\mathcal{C}_2} dz (z-x) \omega_k(z) = 2\pi i x(1-x) \frac{dF(x)}{dx}, \quad (\text{A.25})$$

where we introduced

$$F(x) \equiv {}_2F_1(k/n, 1 - k/n; 1; x). \quad (\text{A.26})$$

From the two equations (A.21) for \mathcal{C}_1 and \mathcal{C}_2 , eliminating $B(x, \bar{x})$ and solving for $A(x, \bar{x})$ we get

$$A(x, \bar{x}) = x(1-x) \frac{d \ln I(x, \bar{x})}{dx}, \quad (\text{A.27})$$

with

$$I(x, \bar{x}) \equiv F(x)\bar{F}(1-\bar{x}) + \bar{F}(\bar{x})F(1-x) = 2\beta(x)|F(x)|^2, \quad (\text{A.28})$$

and we also introduced

$$\tau(x) \equiv \alpha(x) + i\beta(x) \equiv i\frac{F(1-x)}{F(x)}. \quad (\text{A.29})$$

For $n = 2$, $\tau(x)$ gives the modulus of the torus, which is the covering surface of our Riemann sphere with four branch points, but for higher values of n this is not true anymore and (A.29) has no geometric meaning. $A(x, \bar{x})$ gives the desired quantum partition function

$$Z_{\text{qu}}(x, \bar{x}) = \frac{\text{const}}{|x(1-x)|^{4\Delta_{k/n}}} \frac{1}{I(x, \bar{x})}. \quad (\text{A.30})$$

When this equation is specialized to x real, it gives exactly the result anticipated in the main text in Eq. (40).

For the classical part, we only need to construct the properly normalised classical solutions. From the equations of motion, one easily sees that $\partial_z X_{\text{cl}}$ and $\partial_z \bar{X}_{\text{cl}}$ are holomorphic while $\partial_{\bar{z}} X_{\text{cl}}$ and $\partial_{\bar{z}} \bar{X}_{\text{cl}}$ are antiholomorphic and they can be written as

$$\begin{aligned} \partial_z X_{\text{cl}}(z) &= a\omega_k(z), & \partial_{\bar{z}} X_{\text{cl}}(\bar{z}) &= b\bar{\omega}_{n-k}(\bar{z}), \\ \partial_z \bar{X}_{\text{cl}}(z) &= \tilde{a}\omega_{n-k}(z), & \partial_{\bar{z}} \bar{X}_{\text{cl}}(\bar{z}) &= \tilde{b}\bar{\omega}_k(\bar{z}), \end{aligned} \quad (\text{A.31})$$

where $\omega_k(z)$ is given in Eq. (A.14).

The complex constants a , \tilde{a} , b and \tilde{b} are fixed through the global monodromy conditions (A.7) for the closed loops \mathcal{C}_1 and \mathcal{C}_2 . (We do not adopt here the notation of [13], where $\bar{a} \equiv \tilde{a}$ and $\bar{b} \equiv \tilde{b}$, because we find it misleading.) In order to write them, one constructs two classical solutions $X_{\text{cl},1}$ and $X_{\text{cl},2}$ having the following simple global monodromy conditions

$$\Delta_{\mathcal{C}_i} X_{\text{cl},j} = \Delta_{\mathcal{C}_i} \bar{X}_{\text{cl},j} = 2\pi\delta_{ij}, \quad i, j = 1, 2, \quad (\text{A.32})$$

and finds out the corresponding complex constants a_i , \tilde{a}_i , b_i and \tilde{b}_i , which read

$$a_1 = -e^{2\pi i \frac{k}{n}} \tilde{a}_1 = -ie^{\pi i \frac{k}{n}} \frac{\bar{F}(1-\bar{x})}{I(x, \bar{x})}, \quad a_2 = \tilde{a}_2 = -i \frac{\bar{F}(\bar{x})}{I(x, \bar{x})}, \quad (\text{A.33})$$

$$b_1 = -e^{2\pi i \frac{k}{n}} \tilde{b}_1 = -ie^{\pi i \frac{k}{n}} \frac{F(1-x)}{I(x, \bar{x})}, \quad b_2 = \tilde{b}_2 = +i \frac{F(x)}{I(x, \bar{x})}. \quad (\text{A.34})$$

Then, from (A.7) for \mathcal{C}_1 and \mathcal{C}_2 and (A.8), one gets the complex coefficients for X_{cl} to use in (A.31), which read

$$a = a_1 v_1 + a_2 v_2, \quad b = b_1 v_1 + b_2 v_2, \quad (\text{A.35})$$

$$\tilde{a} = \tilde{a}_1 \bar{v}_1 + \tilde{a}_2 \bar{v}_2, \quad \tilde{b} = \tilde{b}_1 \bar{v}_1 + \tilde{b}_2 \bar{v}_2, \quad (\text{A.36})$$

with the vectors characterizing the global monodromy condition of $X_{\text{cl},1}$ and $X_{\text{cl},2}$ given by

$$v_{1,2} \in (1-\theta)\Lambda. \quad (\text{A.37})$$

The last step we need for our purposes is the expression for S_{cl} . By employing the following integral

$$\int |\omega_k|^2 d^2 z = \int \frac{d^2 z}{|z|^{2\frac{k}{n}} |z-x|^{2(1-\frac{k}{n})} |z-1|^{2\frac{k}{n}}} = \frac{\pi^2}{\sin(\pi k/n)} I(x, \bar{x}), \quad (\text{A.38})$$

one finds that

$$S_{\text{cl}}(v_1, v_2) = \frac{\pi \sin(\pi k/n)}{\beta} \left[|\xi_1|^2 |\tau|^2 + \alpha (\xi_1 \bar{\xi}_2 \bar{\gamma} + \bar{\xi}_1 \xi_2 \gamma) + |\xi_2|^2 \right], \quad (\text{A.39})$$

where $\gamma \equiv -ie^{-i\pi k/n}$ and we introduced the vectors ξ_j ($j = 1, 2$) independent of k/n that are generic vectors of the target space lattice Λ , having therefore $v_j = (1 - \theta)\xi_j$.

When we specialize to the problem with real $x \in (0, 1)$, some simplifications occur in the formulas. τ is purely imaginary (i.e. $\alpha = 0$) and $I(x, x) = 2F(x)F(1-x)$. Then Eq. (A.39) reduces to Eq. (42) in the main text, where we restored all the k and n dependence in each quantity.

Appendix B. A transformation formula for the Riemann-Siegel theta function

The Riemann-Siegel theta function $\Theta(0|T)$ for any symmetric complex matrix T with positive imaginary part can be re-written as

$$\Theta(0|T) = \sum_{m \in \mathbf{Z}^g} e^{i\pi m^\dagger \cdot T \cdot m} = \int d^g s \sum_{m \in \mathbf{Z}^g} \delta_g(s - m) e^{i\pi s^\dagger \cdot T \cdot s}. \quad (\text{B.1})$$

Now we employ the following identity (which is a special case of the Poisson resummation formula)

$$\sum_{m \in \mathbf{Z}^g} \delta_g(s - m) = \sum_{j \in \mathbf{Z}^g} e^{2\pi i j^\dagger \cdot s}. \quad (\text{B.2})$$

Plugging (B.2) into (B.1) and inverting $\int d^g s$ and $\sum_{j \in \mathbf{Z}^g}$ in (B.1), we get a g dimensional gaussian integral, which gives

$$\Theta(0|T) = \frac{\Theta(0| -T^{-1})}{\sqrt{\det(-iT)}}. \quad (\text{B.3})$$

Now, by applying this formula for $T = \lambda \tilde{\Gamma} = -A^\dagger(\Gamma/\lambda)^{-1}A$, where $A \equiv 2\hat{U}^\dagger H \hat{U}$ with $H = \text{diag}(\dots, \sin(\pi k/n), \dots)$, we get

$$\Theta(0|\eta \tilde{\Gamma}) = \sqrt{\det(\Gamma/(i\eta))} \Theta(0|A^{-1}(\Gamma/\eta)A^{-1}), \quad (\text{B.4})$$

where we have used that $A^\dagger = A$ and $\det A = 1$ (here A and Γ are the matrix defined in the main text). We employ the following identity

$$\Theta(0|A^{-1}(\Gamma/\eta)A^{-1}) = \Theta(0|\Gamma/\eta), \quad (\text{B.5})$$

which is numerically true, but we give here without a proof. Putting everything together we have

$$\Theta(0|\eta \tilde{\Gamma}) = \frac{1}{\eta^{\frac{n-1}{2}}} \left(\prod_{k=1}^{n-1} \beta_{k/n} \right)^{1/2} \Theta(0|\Gamma/\eta), \quad (\text{B.6})$$

which is exactly Eq. (59) we wanted to prove.

Appendix C. A Thomae-type formula for singular \mathbf{Z}_n curves

In this appendix we employ a Thomae-type formula obtained in [36] for singular \mathbf{Z}_n curves to prove equation (61). In [36], the following singular \mathbf{Z}_n curves $\mathcal{C}_{n,m}$ are considered

$$w^n = p(z)q(z)^{n-1}, \quad p(z) \equiv \prod_{j=0}^m (z - z_{2j+1}), \quad q(z) \equiv \prod_{j=1}^m (z - z_{2j}). \quad (\text{C.1})$$

They have singularities at the points $P_2 = (z_2, 0), \dots, P_{2m} = (z_{2m}, 0)$, while $P_1 = (z_1, 0), \dots, P_{2m+1} = (z_{2m+1}, 0), P_{2m+2} = P_\infty = (\infty, \infty)$ are the branch points. These curves are n sheeted coverings of the complex plane and they define Riemann surfaces of genus $(n-1)m$. The cycles α_k and β_k ($k = 1, \dots, (n-1)m$) (generalizations of \mathcal{C}_1 and \mathcal{C}_2 in Fig. A1 for the many intervals situation, see Ref. [36] for a pictorial representation) provide the basis of the closed loops. We also introduce

$$du_{j+(k-1)m} \equiv \frac{z^{j-1} q(z)^{k-1}}{\mu^k} dz, \quad j = 1, \dots, m, \quad k = 1, \dots, n-1, \quad (\text{C.2})$$

which are a basis of the canonical holomorphic differentials. The $(n-1)m \times (n-1)m$ matrices \mathcal{A} of the α -periods and \mathcal{B} of the β -periods, whose elements read

$$\mathcal{A}_{st} \equiv \oint_{\alpha_s} du_t, \quad \mathcal{B}_{st} \equiv \oint_{\beta_s} du_t, \quad s, t = 1, \dots, (n-1)m, \quad (\text{C.3})$$

respectively, can be written in terms of the following $m \times m$ matrices ($k = 1, \dots, n-1$)

$$(\mathcal{A}_k)_{ij} \equiv \oint_{\alpha_i} du_{j+m(k-1)}, \quad (\mathcal{B}_k)_{ij} \equiv \oint_{\beta_i} du_{j+m(k-1)}, \quad i, j = 1, \dots, m, \quad (\text{C.4})$$

as follows

$$\mathcal{A} = \text{diag}(\mathcal{A}_1, \dots, \mathcal{A}_{n-1}) \mathcal{R}_{\mathcal{A}}, \quad \mathcal{B} = \text{diag}(\mathcal{B}_1, \dots, \mathcal{B}_{n-1}) \mathcal{R}_{\mathcal{B}},$$

where $\text{diag}(\mathcal{A}_1, \dots, \mathcal{A}_{n-1})$ and $\text{diag}(\mathcal{B}_1, \dots, \mathcal{B}_{n-1})$ are block diagonal. The matrices $\mathcal{R}_{\mathcal{A}}$ and $\mathcal{R}_{\mathcal{B}}$ are defined as $\mathcal{R}_{\mathcal{A}} = \tilde{\mathcal{R}}_{\mathcal{A}} \otimes \text{id}_m$ and $\mathcal{R}_{\mathcal{B}} = \tilde{\mathcal{R}}_{\mathcal{B}} \otimes \text{id}_m$ (id_m is the $m \times m$ identity matrix), where the $(n-1) \times (n-1)$ matrices $\tilde{\mathcal{R}}_{\mathcal{A}}$ and $\tilde{\mathcal{R}}_{\mathcal{B}}$ have the following elements

$$(\tilde{\mathcal{R}}_{\mathcal{A}})_{kr} \equiv \rho^{k(1-r)}, \quad (\tilde{\mathcal{R}}_{\mathcal{B}})_{kr} \equiv \frac{\rho^k}{1-\rho^k} (\rho^{-kr} - 1), \quad \rho \equiv e^{\frac{2\pi i}{n}}. \quad (\text{C.5})$$

Introducing the normalised holomorphic differentials $d\vec{v} = (dv_1, \dots, dv_{(n-1)m}) = d\vec{u} \mathcal{A}^{-1}$, allows to define the Riemann period matrix as

$$\Pi_{st} \equiv \oint_{\beta_s} dv_t, \quad s, t = 1, \dots, (n-1)m, \quad (\text{C.6})$$

which turns out to be

$$\Pi = \mathcal{R}_{\mathcal{A}}^{-1} \text{diag}(\mathcal{A}_1^{-1} \mathcal{B}_1, \dots, \mathcal{A}_{n-1}^{-1} \mathcal{B}_{n-1}) \mathcal{R}_{\mathcal{B}}. \quad (\text{C.7})$$

Given these definitions, in [36] the following *Thomae-type formula* (see (5.28) of [36]) has been proven

$$\Theta^8(0|\Pi) = \prod_{k=1}^{n-1} \left[\frac{\det \mathcal{A}_k}{(2\pi i)^m} \right]^4 \prod_{1 \leq i < j \leq m} (z_{2i} - z_{2j})^{2(n-1)} \prod_{0 \leq i < j \leq m} (z_{2i+1} - z_{2j+1})^{2(n-1)}. \quad (\text{C.8})$$

In our case, we have $m = 1$ i.e. four points z_1, z_2, z_3 , and z_4 ; thus $p(z) = (z - z_1)(z - z_3)$ and $q(z) = (z - z_2)(z - z_4)$. In the rhs of (C.8), the product of $(z_{2i} - z_{2j})$ is 1 because $1 \leq i < j \leq 1$ cannot be fulfilled, while the product of $(z_{2i+1} - z_{2j+1})$ has only one term, which is 1. The two independent cycles α_1 and β_1 coincide respectively with \mathcal{C}_1 and \mathcal{C}_2 in Fig. A1. The matrices \mathcal{A}_k are one-by-one, and therefore

$$\Pi = \mathcal{R}_{\mathcal{A}}^{-1} \text{diag}(\mathcal{B}_1/\mathcal{A}_1, \dots, \mathcal{B}_{n-1}/\mathcal{A}_{n-1}) \mathcal{R}_{\mathcal{B}}.$$

Moreover, $\mathcal{R}_{\mathcal{A}} = \tilde{\mathcal{R}}_{\mathcal{A}}$ and $\mathcal{R}_{\mathcal{B}} = \tilde{\mathcal{R}}_{\mathcal{B}}$ and (C.2) reduces to $du_k(z) = \omega_k(z)dz$. Thus, we have that \mathcal{A}_k and \mathcal{B}_k are given by the integrals in Eqs. (A.22). We have the following expression for Π

$$\Pi = \tilde{\mathcal{R}}_{\mathcal{A}}^{-1} \text{diag}(\dots, \rho^{k/2} \beta_{k/n}, \dots) \tilde{\mathcal{R}}_{\mathcal{B}}. \quad (\text{C.9})$$

By introducing the $(n-1) \times (n-1)$ matrix M_1 having all the elements equal to 1, we can write $\tilde{\mathcal{R}}_{\mathcal{A}}^{-1}$ and $\tilde{\mathcal{R}}_{\mathcal{B}}$ in terms of the matrix \hat{U} as follows

$$\tilde{\mathcal{R}}_{\mathcal{A}}^{-1} = \frac{1}{\sqrt{n}} (\text{id}_{n-1} + M_1) \hat{U} \text{diag}(\dots, \rho^{-k}, \dots), \quad (\text{C.10})$$

$$\tilde{\mathcal{R}}_{\mathcal{B}} = \sqrt{n} \text{diag} \left(\dots, \frac{\rho^k}{1 - \rho^k}, \dots \right) \hat{U}^\dagger (\text{id}_{n-1} + M_1). \quad (\text{C.11})$$

Now we observe that the matrix (C.9) is related to Γ of Eq. (9) as

$$\Pi = A^{-1} \Gamma A^{-1}, \quad (\text{C.12})$$

where $A \equiv 2\hat{U}^\dagger H \hat{U}$ with $H = \text{diag}(\dots, \sin(\pi k/n), \dots)$. As for the rhs of (C.8), it reduces to (notice that $\prod_{k=1}^{n-1} \rho^{k/2} = (-i)^{n-1}$)

$$\prod_{k=1}^{n-1} \left(\frac{\mathcal{A}_k}{2\pi} \right)^4 = \left(\prod_{k=1}^{n-1} {}_2F_1(k/n, 1 - k/n; 1; x) \right)^4. \quad (\text{C.13})$$

Using finally $\Theta(0|A^{-1} \Gamma A^{-1}) = \Theta(0|\Gamma)$ Eq. (B.5), we have therefore proved (61).

Appendix D. Three analytic continuations more

Appendix D.1. The analytic case $x = 1/2$

For $x = 1/2$, the hypergeometric function can be written in terms of Γ function as

$$F_{k/n}(1/2) = \frac{\sqrt{\pi}}{\Gamma(1 - k/(2n))\Gamma(k/(2n) + 1/2)}, \quad (\text{D.1})$$

so that the D_n simplifies to

$$D_n(1/2) = \log \prod_{k=1}^{n-1} F_{k/n}(1/2) = \log \frac{\pi^{(n-1)/2}}{\prod_{l=1}^{n-1} [\Gamma(1/2 + l/(2n))]^2}. \quad (\text{D.2})$$

We can then employ the following integral representation of the logarithm of the Γ function

$$\log \Gamma(z) = \int_0^\infty \frac{dte^{-t}}{t} \left(\frac{e^{-(z-1)t} - 1}{1 - e^{-t}} + z - 1 \right), \quad (\text{D.3})$$

and so

$$\log \Gamma \left(\frac{1}{2} + \frac{l}{2n} \right) = \int_0^\infty \frac{dte^{-t}}{t} \left(\frac{e^{-(l/(2n)-1/2)t} - 1}{1 - e^{-t}} + \frac{l}{2n} - \frac{1}{2} \right), \quad (\text{D.4})$$

The resulting series is easily summed

$$D_n(1/2) = \frac{n-1}{2} \ln \pi - 2 \int_0^\infty \frac{dt e^{-t}}{t} \left(\frac{e^t(e^{t/2} - 1 - n(e^{t/(2n)} - 1))}{(e^t - 1)(e^{t/(2n)} - 1)} + \frac{1-n}{4} \right), \quad (\text{D.5})$$

and the derivative wrt n taken

$$D'_1(1/2) = -\frac{1}{2} \ln \pi + \int_0^\infty \frac{dt e^{-t}}{2t} \frac{e^{3t/2}(2t-5) + 5e^t + e^{t/2} - 1}{(e^t - 1)(e^{t/2} - 1)}. \quad (\text{D.6})$$

The integral is convergent, but the various pieces in which it can be divided are not and so a lot of care must be used to perform it. The easiest way we find out to make the integral is to make a sort of dimensional regularization of the term $t^{-1} \rightarrow t^{-1+\nu}$, making then the various integrals that are finite for large enough ν and then expanding the result close to $\nu = 0$ where all the divergences cancel leaving (after long algebra) the finite result

$$D'_1(1/2) = \frac{1}{2}(-1 - \gamma_E + \ln \pi) \simeq -0.216243, \quad (\text{D.7})$$

where γ_E is the Euler γ constant.

Appendix D.2. Perturbative expansion in x

The easiest way to perform the analytic continuation is to expand in power of x the function $F_{k/n}(x)$. From the well-known series of the hypergeometric function the coefficient of this expansion at order p is a polynomial of order $2p$ in k/n . The product over k from 1 to $n-1$ can be done for very large orders and the derivative for $n=1$ taken. With a little help from Mathematica we obtain the following perturbative series for $D'_1(x)$:[‡]

$$\begin{aligned} -D'_1(x) &= \frac{x}{3} + \frac{2}{15}x^2 + \frac{26}{315}x^3 + \frac{2}{35}x^4 + \frac{52}{1155}x^5 + \frac{302}{9009}x^6 + \frac{76}{2145}x^7 + \frac{398}{255255}x^8 \\ &\quad + \frac{327128}{2297295}x^9 - \frac{18047684}{24249225}x^{10} + \frac{31378136}{5311735}x^{11} + O(x^{12}). \end{aligned} \quad (\text{D.8})$$

It is easy to obtain as many terms of this series as we want, but this is useless if we perform a direct summation. In fact, it is evident that the terms up x^8 are all positive and quickly decreasing in magnitude, giving the impression of a convergent series. Unfortunately from the term x^9 they start increasing abruptly and oscillating signaling that $D'_1(x)$ is an asymptotic series. It would be possible to resum this series a'la Borel, but this is of no use in view of the exact result we obtained in the main text. This result, that is very easy to obtain, has been a fundamental cross-check for other relations we found. It also provides a very good estimation of $D'_1(x)$ for $x \leq 1/2$. For example, summing the first eight terms for $x = 1/2$ we obtain $D'_1(1/2) \sim -0.216102$, deviating only of the 0.06% from the exact result above.

[‡] A numerology digression: The denominators in this Taylor series are integer multiple of the ones of $\tan x$ up to order 10 when $D'_1(x)$ starts oscillating. On the Sloane on-line encyclopedia of integer sequences, another “look-a-like the denominators in Taylor series for $\tan x$ ” can be found, (sequence number A156769) that starts differentiating from $\tan x$ at the eleventh term (excluding x), exactly like this one.

Appendix D.3. Analytic continuation for small x

In this appendix we report the details of the analytic continuation in the small x regime. We need to continue to general complex n the sum P_n in Eq. (83). It is instructive to consider first two special cases that are easily worked out. For $\alpha = 1$ we have

$$P_n = \sum_{l=1}^{n-1} \frac{l/n}{[\sin(\pi l/n)]^2} = \frac{1}{6}(n^2 - 1), \quad (\text{D.9})$$

so that $P'_1 = 1/3$ (but we remember that this number has no physical meaning, because it is exactly canceled by the denominator to give $\mathcal{F}'_1(x) = 0$).

The other easily solvable case is $\alpha = 1/2$, for which we have

$$P_n = \sum_{l=1}^{n-1} \frac{l/n}{\sin(\pi l/n)}. \quad (\text{D.10})$$

We can use

$$\int_0^\infty \frac{x^\mu}{(1+x)^2} dx = \frac{\pi\mu}{\sin \pi\mu} \quad (\text{D.11})$$

with $\mu = l/n$, to have

$$\begin{aligned} P_n &= \frac{1}{\pi} \int_0^\infty \frac{dx}{(1+x)^2} \sum_{l=1}^{n-1} x^{l/n} = \frac{1}{\pi} \int_0^\infty \frac{dx}{(1+x)^2} \frac{x - x^{1/n}}{x^{1/n} - 1} \\ &= \frac{n}{\pi} \int_0^\infty (\coth x \tanh(nx) - 1) dx, \end{aligned} \quad (\text{D.12})$$

that is the desired analytic continuation. From this we have

$$P'_1 = \frac{1}{\pi} \int_0^\infty \frac{x \ln x}{(x-1)(1+x)^2} dx = \frac{1}{\pi} \int_0^\infty \frac{x}{\sinh x \cosh x} dx = \frac{\pi}{8}. \quad (\text{D.13})$$

It is also possible to give other simple formulas for all integer values of 2α , but they are not values of physical interest. Let us just mention that for $\alpha = 0$ we trivially have $P_n = (n-1)/2$ with $P'_1 = 1/2$.

For general $0 < \alpha < 1$, the only strategy we found is to expand the argument of the sum using

$$\frac{x}{(\sin x)^\mu} = x^{1-\mu} \sum_{k=0}^{\infty} p_k x^{2k}, \quad (\text{D.14})$$

with p_k known (also to Mathematica). Using this expansion we have

$$\begin{aligned} P_n &= \frac{1}{\pi} \sum_{l=1}^{n-1} \frac{\pi l/n}{[\sin(\pi l/n)]^{2\alpha}} = \frac{1}{\pi} \sum_{k=0}^{\infty} p_k \left(\frac{\pi}{n}\right)^{1+2(k-\alpha)} \sum_{l=1}^{n-1} l^{1+2(k-\alpha)} \\ &= \frac{1}{\pi} \sum_{k=0}^{\infty} p_k \left(\frac{\pi}{n}\right)^{1+2(k-\alpha)} H_{n-1}^{(-2(k-\alpha)-1)}, \end{aligned} \quad (\text{D.15})$$

where the harmonic number $H_r^{(\mu)}$ is the natural analytic continuation of the above sum (defined e.g. in terms of the Riemann ζ as $H_z^{(\mu)} = \zeta(\mu) - \zeta(\mu, z+1)$). This sum is still not analytically possible, and does not provide a proper analytic continuation yet. In fact, it is easy to check that only for integer n it gives a convergent sum (that can

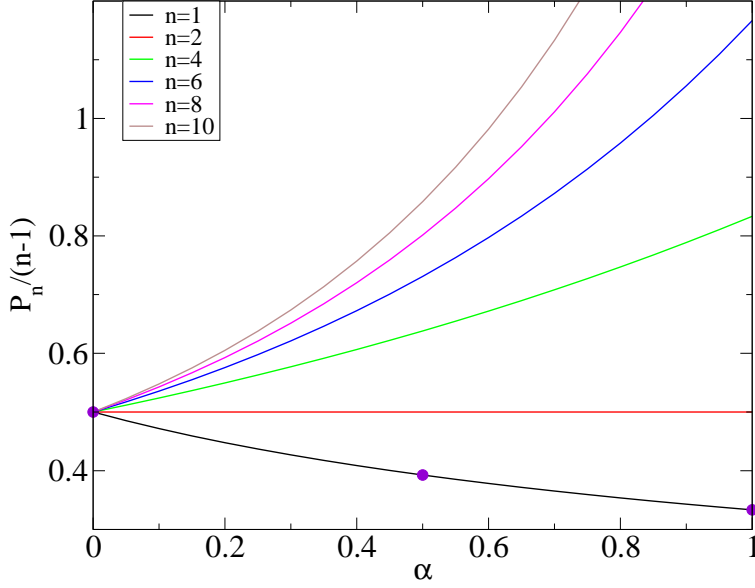


Figure D1. $P_n/(n-1)$ as function of $\alpha = \min(\eta, 1/\eta)$ for several integral n and the analytic continuation to $n \rightarrow 1$ needed for the entanglement entropy (lowest curve). The large points are for the three values known analytically (they perfectly agree with the numerical computation, confirming its correctness).

be simply truncated at a given order to have the desired precision). For non-integral values, the sum is asymptotic and must be resummed. We explicitly show how to do this only for P'_1 needed for the entanglement entropy. Taking the derivative wrt to n , we formally get

$$P'_1 = \sum_{k=0}^{\infty} p_k \pi^{2(k-\alpha)} (1 - 2(k-\alpha)) \zeta(2(\alpha-k)). \quad (\text{D.16})$$

This sum is asymptotic. We then introduce the function

$$\mathcal{P}(z) = \sum_{k=0}^{\infty} p_k z^{2(k-\alpha)} (1 - 2(k-\alpha)) \zeta(2(\alpha-k)) \equiv \sum_{k=0}^{\infty} P_k z^{2(k-\alpha)}, \quad (\text{D.17})$$

with the coefficient P_k growing like a factorial for large k . By definition we have $P'_1 = \mathcal{P}(\pi)$. The α -Borel transform is

$$B_{\mathcal{P}}(t) = \sum_{k=0}^{\infty} \frac{P_k}{\Gamma(2(k-\alpha+1))} t^{2(k-\alpha)}, \quad (\text{D.18})$$

that provides a convergent sum. In case we would have been able to perform this sum analytically, the original function would be given by the anti-Borel transform

$$\mathcal{P}(z) = \frac{1}{z} \int_0^{\infty} e^{-t/z} t^{-2\alpha} B_{\mathcal{P}}(t) dt, \quad (\text{D.19})$$

as it can be checked by expanding in z . (We used the α -Borel transform to cancel the effect of the singularity of the Borel transform in the origin, however this has no importance for the numerical results). The analytic sum can not be performed, and so one should find an effective approximation of the sum (D.18) that makes the

integral (D.19) finite. There are several standard methods to do this and we use the Padè approximation of the series, that is a ratio of polynomial of order N and D for numerator and denominator respectively. We consider in the integral (D.19) large enough N and D , so that the value of P'_1 does not change (at the required accuracy) when still increasing them. Within this procedure we got the values of P'_1 for any $0 < \alpha < 1$ that are reported in the Fig. D1 together with $P_n/(n-1)$ for integer n .

References

- [1] L. Amico, R. Fazio, A. Osterloh, and V. Vedral, Entanglement in Many-Body Systems, *Rev. Mod. Phys.* **80**, 517 (2008) [quant-ph/0703044].
- [2] J. Eisert, M. Cramer, and M. B. Plenio, Area laws for the entanglement entropy - a review, *Rev. Mod. Phys.* **XX**, XXX (2009) [0808.3773].
- [3] P. Calabrese and J. Cardy, Entanglement entropy and conformal field theory, *J. Phys. A*, to appear [0905.4013].
- [4] Entanglement entropy in extended systems, P. Calabrese, J. Cardy, and B. Doyon Eds., *J. Phys. A*, Special issue, in preparation.
- [5] C. Holzhey, F. Larsen, and F. Wilczek, Geometric and Renormalized Entropy in Conformal Field Theory, *Nucl. Phys. B* **424**, 443 (1994) [hep-th/9403108].
- [6] G. Vidal, J. I. Latorre, E. Rico, and A. Kitaev, Entanglement in quantum critical phenomena, *Phys. Rev. Lett.* **90**, 227902 (2003) [quant-ph/0211074]
J. I. Latorre, E. Rico, and G. Vidal, Ground state entanglement in quantum spin chains, *Quant. Inf. and Comp.* **4**, 048 (2004) [quant-ph/0304098].
- [7] P. Calabrese and J. Cardy, Entanglement entropy and quantum field theory, *J. Stat. Mech.* P06002 (2004) [hep-th/0405152].
- [8] P. Calabrese and J. Cardy, Entanglement entropy and quantum field theory: a non-technical introduction, *Int. J. Quant. Inf.* **4**, 429 (2006) [quant-ph/0505193].
- [9] S. Furukawa, V. Pasquier, and J. Shiraishi, Mutual Information and Compactification Radius in a $c=1$ Critical Phase in One Dimension, *Phys. Rev. Lett.* **102**, 170602 (2009) [0809.5113].
- [10] B. Hsu, M. Mulligan, E. Fradkin, and E.-A. Kim, Universal entanglement entropy in 2D conformal quantum critical points, *Phys. Rev. B* **79**, 115421 (2009) [0812.0203];
J.-M. Stephan, S. Furukawa, G. Misguich, and V. Pasquier; Shannon and entanglement entropies of one- and two-dimensional critical wave functions, [0906.1153].
- [11] M. Caraglio and F. Gliozzi, Entanglement Entropy and Twist Fields, *JHEP* 0811: 076 (2008) [0808.4094].
- [12] P. Di Francesco, P. Mathieu, and D. Senechal, *Conformal Field Theory* (Springer-Verlag, New York, 1997).
- [13] L. J. Dixon, D. Friedan, E. J. Martinec and S. H. Shenker, The Conformal Field Theory of Orbifolds, *Nucl. Phys. B* **282** (1987) 13.
- [14] A.I. B. Zamolodchicov, Conformal scalar field on the hyperelliptic curve and critical Ashkin-Teller multipoint correlation functions, *Nucl. Phys. B* **285** (1987) 481.
- [15] H. Wichterich, J. Molina-Vilaplana, and S. Bose, Scale invariant entanglement at quantum phase transitions, *Phys. Rev. A* **80**, 010304(R) (2009) [0811.1285].
- [16] S. Marcovitch, A. Retzker, M. B. Plenio, and B. Reznik, Critical and noncritical long range entanglement in the Klein-Gordon field, *Phys. Rev. A* **80**, 012325 (2009) [0811.1288].
- [17] J. L. Cardy, O.A. Castro-Alvaredo, and B. Doyon, Form factors of branch-point twist fields in quantum integrable models and entanglement entropy, *J. Stats. Phys.* **130** (2007) 129 [0706.3384].
- [18] V. G. Knizhnik, Analytic fields on Riemann surfaces. II, *Commun. Math. Phys.* **112**, 567 (1987).
- [19] M. Bershadsky and A. Radul, Conformal field theories with additional Z_N symmetry, *Int. J. Mod. Phys. A* **2**, 165 (1987).
- [20] R. Dijkgraaf, E. Verlinde, and H. Verlinde, $c = 1$ conformal field theories on Riemann surfaces, *Commun. Math. Phys.* **115**, 649 (1988);
K. Miki, Vacuum amplitudes without twist fields for $Z(N)$ orbifold and correlation functions of twist fields for $Z(2)$ orbifold, *Phys. Lett. B* **191** (1987) 127;
L. Alvarez-Gaume, G. W. Moore and C. Vafa, Theta functions, modular invariance, and strings, *Commun. Math. Phys.* **106**, 1 (1986);
L. Alvarez-Gaume, J. B. Bost, G. W. Moore, P. C. Nelson and C. Vafa, Bosonization on

- higher genus Riemann surfaces, *Commun. Math. Phys.* **112** (1987) 503;
 D. Bernard, Z_2 -twisted fields and bosonization on Riemann surfaces, *Nucl. Phys. B* **302** (1988) 251;
 J. J. Atick, L. J. Dixon, P. A. Griffin and D. Nemeschansky, Multiloops twist field correlation functions for $Z(N)$ orbifolds, *Nucl. Phys. B* **298** (1988) 1.
- [21] A. A. Belavin, A. M. Polyakov and A. B. Zamolodchikov, Infinite conformal symmetry in two-dimensional quantum field theory, 1984 *Nucl. Phys. B* **241** 333.
- [22] P. Calabrese, M. Campostrini, and B. Nienhuis, to appear.
- [23] B. Nienhuis, M. Campostrini, and P. Calabrese, Entanglement, combinatorics and finite-size effects in spin-chains, *J. Stat. Mech.* (2009) P02063 [0808.2741].
- [24] H. Casini and M. Huerta, A finite entanglement entropy and the c-theorem, *Phys. Lett. B* **600** (2004) 142 [hep-th/0405111].
- [25] H. Casini, C. D. Fosco, and M. Huerta, Entanglement and alpha entropies for a massive Dirac field in two dimensions, *J. Stat. Mech.* P05007 (2005) [cond-mat/0505563].
- [26] H. Casini and M. Huerta, Remarks on the entanglement entropy for disconnected regions, *JHEP* 0903: 048 (2009) [0812.1773].
- [27] H. Casini and M. Huerta, Reduced density matrix and internal dynamics for multicomponent regions, *Class. Quant. Grav.* **26**, 185005 (2009) [0903.5284].
- [28] P. Facchi, G. Florio, C. Invernizzi, and S. Pascazio, Entanglement of two blocks of spins in the critical Ising model, *Phys. Rev. A* **78**, 052302 (2008) [0808.0600].
- [29] I. Klich and L. Levitov, Quantum Noise as an Entanglement Meter, *Phys. Rev. Lett.* **102**, 100502 (2009) [0804.1377].
- [30] S. Ryu and T. Takayanagi, Holographic Derivation of Entanglement Entropy from AdS/CFT, *Phys. Rev. Lett.* **96** (2006) 181602 [hep-th/0603001];
 S. Ryu and T. Takayanagi, Aspects of Holographic Entanglement Entropy, *JHEP* 0608: 045 (2006) [hep-th/0605073];
 T. Nishioka, S. Ryu, and T. Takayanagi, Holographic Entanglement Entropy: An Overview, 0905.0932.
- [31] V. E. Hubeny and M. Rangamani, Holographic entanglement entropy for disconnected regions, *JHEP* 0803: 006 (2008) [0711.4118].
- [32] P. Calabrese and J. Cardy, Evolution of Entanglement entropy in one dimensional systems, *J. Stat. Mech.* P04010 (2005) [cond-mat/0503393].
- [33] P. Calabrese and J. Cardy, Entanglement and correlation functions following a local quench: a conformal field theory approach, *J. Stat. Mech.* (2007) P10004 [0708.3750].
- [34] P. Calabrese and A. Lefevre, Entanglement spectrum in one-dimensional systems, *Phys. Rev. A* **78**, 032329 (2008) [0806.3059].
- [35] V. Alba, L. Tagliacozzo, and P. Calabrese, Entanglement entropy of two disjoint blocks in critical Ising models, [0910.0706].
- [36] V. Z. Enolski and T. Grava, Singular Z_n curves, Riemann-Hilbert problem and Schlesinger equations, math-ph/0306050;
 V. Z. Enolski and T. Grava, Thomae type formulae for singular Z_n curves, *Lett. Math. Phys.* **76** (2006) 187 [math-ph/0602017].